Diffusion-Driven Mechanisms of Protein Translocation on Nucleic Acids. 3. The *Escherichia coli lac* Repressor–Operator Interaction: Kinetic Measurements and Conclusions†

Robert B. Winter,‡ Otto G. Berg,§ and Peter H. von Hippel*

ABSTRACT: The association and dissociation kinetics of the *Escherichia coli lac* repressor–operator (RO) complex have been examined as a function of monovalent ion concentration and operator-containing DNA fragment length in order to investigate the mechanisms used by repressor in locating (and dissociating from) the operator site. Association rate constants (k_a) measured with an 80- or a 203-base-pair *lac* operator containing DNA fragment are 3–5-fold smaller than those determined with a 6700-base-pair operator fragment or with intact λp*lac*5 DNA (50 000 base pairs) at all salt concentrations tested. At salt concentrations less than ~0.1 M KCl, association rate constants to all operator-containing DNA fragments (except λp*lac*5 DNA) are insensitive to variations in salt concentration, but the limiting low salt value of k_a appears to depend upon operator-containing DNA length. The value of k_a for λp*lac*5 DNA decreases significantly from the ~0.1 M KCl maximum at low salt. Above ~0.1 M KCl, repressor–operator association rate constants for all operator-containing DNA substrates tested show a similar decrease with increasing salt concentration, which does not appear to depend upon the length of the DNA molecule (except for the very small DNA fragments). In contrast to the association reaction, k_d, the dissociation rate constant, decreases linearly (on a log k_d vs. log [KCl] plot) with decreasing salt concentration over virtually the entire salt concentration range studied (0.05–0.2 M KCl). These results are consistent with the explanation of the unusually fast association kinetics for this system in terms of a two-step model in which repressor initially diffuses to a nonoperator DNA binding site (forming an RD complex) and then rapidly "scans" (in a locally correlated fashion) adjacent sites until the operator is located or the repressor dissociates from the chain. Dissociation of the RO complex follows the same two-step process in reverse. Quantitative comparisons are made between these results and the theoretical predictions of the two facilitating translocation mechanisms (one-dimensional "sliding" along the DNA double helix and direct transfer between DNA segments) developed in the first paper of this series [Berg, O. G., Winter, R. B., & von Hippel, P. H. (1981) *Biochemistry* (first paper of three in this issue)]. We conclude that the experimental data for the "faster-than-diffusion-controlled" interaction of repressor and operator can be quantitatively modeled by a two-step process in which sliding is the dominant transfer mechanism. Molecular models of the initial nonspecific binding event (including "hopping") as well as sliding and interchain transfer are discussed, and the possible roles of facilitated translocation mechanisms of the diffusion-driven type in this and other in vitro and in vivo protein–nucleic acid interaction processes are considered.

In the first paper of this series (Berg et al., 1981), we pointed out that at least in in vitro measurements in dilute solution, certain binding interactions between genome-regulatory proteins and their specific DNA target sequences seemed to proceed at "faster-than-diffusion-controlled" rates. This suggested, of course, that the overall binding reaction must be viewed as a two- (or more) step process, with a free diffusion event to an expanded initial target (perhaps the entire DNA molecule) followed by one or more translocation events of reduced dimensionality or volume resulting in rapid location of the DNA target site by the binding protein. The observed binding of DNA regulatory proteins to sequences other than the target provides the necessary nonspecific affinity to support such facilitating processes, and in Berg et al. (1981) several specific translocation mechanisms have been described and their mathematical properties developed.

Though the models and theory presented in Berg et al. (1981) are general, the only actual system which has so far been sufficiently developed to permit an experimental test of these ideas is the *Escherichia coli lac* repressor–operator-DNA interaction. Theory shows that major and characteristic changes in the association and dissociation kinetics of the repressor–operator complex (RO) may be expected by varying the nonspecific affinity of repressor for DNA (K_{RD}) and by varying the length of the DNA lattice in which the operator is imbedded. Experimentally K_{RD} can be easily (and dramatically) manipulated by varying the salt concentration of the system, and the availability of specific restriction enzymes and the known restriction map makes it easy to produce operator-containing DNA fragments of known length. Since [see Berg et al. (1981)] variations in K_{RD} and lattice length have very different effects on the overall RO association and dissociation kinetics, depending on the magnitude of the contributions to the rates made by the various translocation mechanisms, we have undertaken a systemic experimental study of the effects of these variables on the equilibrium and kinetic parameters of the *lac* system. The equilibrium findings are presented in the immediately preceding paper (Winter & von Hippel, 1981); in this paper we present the kinetic results, and examine the fit of these results to the predictions of theory,

† From the Institute of Molecular Biology and Department of Chemistry, University of Oregon, Eugene, Oregon 97403. *Received April 20, 1981.* A portion of this work was presented by R.B.W. to the Graduate School of the University of Oregon in partial fulfillment of the requirements for the Ph.D. degree in Chemistry. This research was supported in part by U.S. Public Health Service Research Grant GM-15792 (to P.H.v.H.). R.B.W. was a predoctoral trainee on U.S. Public Health Service Training Grants GM-00715 and GM-07759. O.G.B. is grateful for partial support from the Swedish Natural Science Research Council.

‡ Present address: Department of Molecular, Cellular and Developmental Biology, University of Colorado, Boulder, CO 80302.

§ Present address: Department of Theoretical Physics, Royal Institute of Technology, S-100 44 Stockholm, Sweden.

0006-2960/81/0420-6961$01.25/0

in order to attempt to define the translocation processes which actually apply to this system. A parallel study of some aspects of the salt dependence of the equilibrium and kinetics of the *lac* RO interaction has been carried out independently by Barkley (1981) and Barkley et al. (1981). Their results are generally quite complementary to ours and increase our confidence in the reproducibility of the quantitative filter binding technique used in these studies and in the interpretations that result.

Materials and Methods

Materials. The preparation and purification of *lac* repressor and of *lac* operator containing DNA molecules and fragments have been described in the preceding paper (Winter & von Hippel, 1981).

Measurement of RO Association Kinetics. Binding buffers and filtering procedures have been described previously (Winter & von Hippel, 1981). Measurements of association rate constants (k_a) followed closely the procedures developed by Riggs et al. (1970). Reactions were carried out in 1.5–3.0 mL of modified binding buffer (BB) with ^{32}P-labeled operator concentrations of $\sim 1 \times 10^{-12}$ M for the experiments with λp*lac*5 DNA, $(0.5–2) \times 10^{-12}$ M for the experiments with the *Eco*RI *lac* fragment, and 4×10^{-12} M for the studies with the 80-, 170-, and 203-pair *lac* fragments. Active repressor was added to 0.7×10^{-12} M for the experiments with λp*lac*5 DNA, $(1–4) \times 10^{-12}$ M for those with the *Eco*RI *lac* fragment, and 6×10^{-12} M for those with the 80-, 170-, and 203-base-pair fragments. The reaction was generally stopped at the desired times by the addition of a 50-fold excess of unlabeled λp*lac*5 DNA. The measured filter-bound counts per minute (cpm) at all time points were corrected for the amount of DNA retained on the filter in the absence of added repressor (usually ≤5% of the input DNA).

For most experiments, the data have been analyzed in terms of a simple, second-order reaction ($R + O \xrightarrow{K} RO$), since under the conditions used the dissociation reaction is slow enough to be neglected. The integrated rate equation which applies to this condition is

$$\left[\frac{1}{(R) - (O)}\right] \ln \left[\frac{(O)[(R) - (RO)]}{(R)[(O) - (RO)]}\right] = k_a t \quad (1)$$

where (R), (O), and (RO) represent the concentrations of repressor, operator, and complex, respectively. In the kinetic experiments with the short (80-, 170-, and 203-base-pair) *lac* fragments at ≥0.15 M KCl, the dissociation reaction is fast enough so that the entire process (i.e., $R + O \underset{k_d}{\overset{k_a}{\rightleftharpoons}} RO$) must be considered. These data were fitted to the integrated rate equation

$$\frac{1}{\sqrt{-q}}\left[\left(\ln \frac{2k_a(RO) + b - \sqrt{-q}}{2k_a(RO) + b + \sqrt{-q}}\right) - \ln\left(\frac{b - \sqrt{-q}}{b + \sqrt{-q}}\right)\right] = t \quad (2)$$

where $-b = k_a(O) + k_a(R) + k_d$, and $q = 4k_a^2(R)(O) - b^2$.

The conversion of counts per minute to concentrations of repressor–operator complex was carried out by determining the counts per minute retained on filters in equilibrium binding experiments containing 5–10-fold excesses of repressor over operator, to ensure that all the operator DNA had been driven into RO complexes. These values were compared with counts per minute retained on filters at long times in kinetic experiments (>10 min), after equilibrium had been attained, and used in this way to establish "plateau" values of RO concentrations in rate experiments. At shorter times (10–120 s), the product of $(cpm)_t/(cpm)_{plateau}$ and $(RO)_{plateau}$ thus gives the concentration of RO at any time t. Comparisons of counts per minute on filters in equilibrium and kinetic experiments were carried out under identical ionic conditions since the level of radioactivity retained on the filters decreases with increasing salt concentration.

Measurement of RO Dissociation Kinetics. Reactions were carried out by using $(1–3) \times 10^{-11}$ M operator concentrations, with active repressor added to 50% and 75% saturation levels. Reaction volumes were usually 3.0 mL. After incubation for 20–30 min at room temperature, an ~50-fold excess of λp*lac*5 DNA was added at zero time, and 100-μL aliquots were withdrawn and filtered at the desired times. At the end of the experiment isopropyl β-D-thiogalactoside (IPTG) was added to a final concentration of 1 mM, and aliquots were filtered to determine background corrections.

The dissociation data have also been analyzed as an irreversible first-order reaction ($RO \xrightarrow{k_d} R + O$), under conditions where the reassociation rate could be ignored due to the presence of the unlabeled λp*lac*5 DNA used to "trap" the released repressor. The relevant integrated rate equation for these conditions is

$$\ln \frac{(RO)}{(RO)_0} = k_d t \quad (3)$$

where (RO) represents the concentration of RO complex at time t and $(RO)_0$ is the concentration of RO complex determined immediately (within 15 s) after the addition of unlabeled λp*lac*5 DNA.

Results and Discussion

Quantitative Filter Binding Method. It should be pointed out that all experimental measurements of the RO interaction to date (including those reported here and in the preceding paper; Winter & von Hippel, 1981) have been made with the filter binding method, which must be applied and interpreted very carefully to avoid serious systematic error. The actual measure of binding is the retention, on a nitrocellulose filter, of a radioactively labeled DNA molecule, which adheres to the filter via protein tightly bound to it. A number of artifacts must be taken into account; some of these have been described and analyzed by Riggs et al. (1970) in the original paper on the technique as applied to the RO system, as well as by Hinkle & Chamberlin (1972). Among the more serious problems are inefficiency of retention of the labeled macromolecule on the filter, complications due to the binding of more than one protein to specific DNA sites [e.g., two or more operators on one piece of DNA; see Winter & von Hippel (1981)], and retention of DNA on the filter as a consequence of nonspecific binding of repressor to nonoperator DNA. Retention via nonspecific binding can be detected by monitoring RO dissociation in the presence of added inducer (typically IPTG); the nonspecific binding component is not perturbed by inducer. To sort out these subtleties requires the development and use of very reproducible experimental technique, though even then the irreducible standard errors of the method are appreciable.

New and more direct physiochemical techniques for monitoring the RO interaction are being developed in various laboratories, largely because of the increased availability of operator-containing DNA (as a consequence of cloning techniques) and of repressor protein (due to the development of repressor overproducing strains). However, after all these

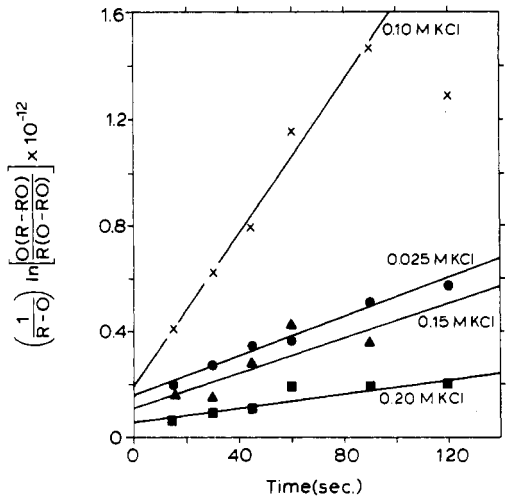

FIGURE 1: Kinetics of the formation of the RO complex with λp*lac*5 DNA at various salt concentrations. Experimental procedures are described under Materials and Methods. The solid lines represent the best linear least-squares fit to the data points, plotted according to eq 1. (●) Binding buffer (BB) + 0.025 M KCl, slope = k_a = 3.5 × 10^9 M^{-1} s^{-1}; (×) BB + 0.10 M KCl, k_a = 1.4 × 10^{10} M^{-1} s^{-1}; (▲) BB + 0.15 M KCl, k_a = 3.3 × 10^9 M^{-1} s^{-1}; (■) BB + 0.20 M KCl, k_a = 1.4 × 10^9 M^{-1} s^{-1}.

drawbacks were conceded, the power of the filter-binding method to monitor interactions involving extremely small amounts of material (picomoles or less) at concentrations of 10^{-12} M should not be underestimated, and great insight, which would not have been possible otherwise, can be (and has been) obtained by these means.

Repressor–Operator Association Kinetics. In order to examine the kinetic pathways by which repressor finds its operator target, we have studied the rate of RO complex formation as a function of salt concentration and of operator-containing DNA fragment size. By varying salt concentration, we have been able to manipulate K_{RD} and thus the length of time a repressor molecule remains bound to nonoperator DNA following a diffusional collision. By varying the *size* of the DNA fragment, we can control the number of vicinal nonspecific sites which must be explored prior to target site location.

The experiments designed to measure RO association rates as a function of salt concentration were carried out by using the following general protocol. Repressor and radioactive (^{32}P-labeled) operator-containing DNA were mixed at zero time in the salt solution of interest. Aliquots were removed, filtered, and washed at various times after mixing to develop the overall association rate curve. Since the overall reaction always appears second order (first order in repressor *and* in operator), the concentrations of these components can be adjusted (within limits; see Materials and Methods) to obtain reaction times convenient for manual manipulation (half-times of the order of minutes).

Association to λplaC5 DNA. In Figure 1 we present several experiments in which the rates of RO association have been determined by using whole λp*lac*5 DNA (50 000 base pairs) at several different KCl concentrations as the operator-containing lattice. The data are plotted in accord with eq 1, for which a straight line indicates that apparent second-order behavior is indeed being followed. The slopes of the lines then correspond to the observed second-order association rate constants (k_a). The experiments were performed as described under Materials and Methods and were carried out in binding buffer (BB) containing no Mg^{2+} or other divalent ions. Figure 1 shows that the rate increases initially with decreasing KCl

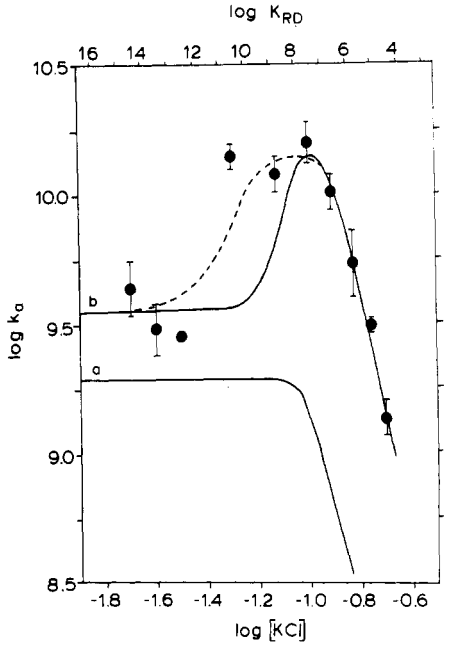

FIGURE 2: Log k_a vs. log [KCl] for RO complex formation with λp*lac*5 DNA (see Materials and Methods). The points represent the experimental data, with error bars indicating the standard deviation for experiments repeated several times. The lines are theoretical and have been calculated as described in Berg et al. (1981) and in the text. The solid curves represent the predicted RO association constants calculated as a function of K_{RD} (upper abscissa) estimated by using eq 13. The parameter values used are D = 5 × 10^{-7} cm^2/s, M = 5 × 10^4 base pairs, R_c = 1200 Å, r_g = 5500 Å, and O_T = 10^{-12} M. Curve a shows the results expected using the intersegment transfer mechanism as the sole translocation mechanism, calculated according to eq 7 and 11 with ν = 100 s^{-1}. Curve b shows the results expected using the sliding mechanism only, according to eq 7 and 12 with D_1 = 9 × 10^{-10} cm^2/s. The dashed portion of curve b is calculated assuming a weaker salt dependence of K_{RD} at low salt (i.e., log K_{RD} = −5 log [KCl] + 2.25 at log [KCl] < −0.95; see also footnote 2).

concentration (from 0.2 to ~0.1 M KCl) and then decreases again at lower salt concentrations.

In Figure 2 these and other values of k_a are plotted against KCl concentration in a log–log form, and the overall behavior of the system becomes clear. We see that log k_a *increases* linearly with log [KCl] as the salt concentration is decreased from 0.2 to ~0.1 M, with k_a increasing ~10-fold over this salt concentration range. At ~0.1 M KCl, k_a reaches a maximum value ($k_a \simeq 2 \times 10^{10}$ M^{-1} s^{-1}) and then decreases again as the salt concentration is lowered further.

Effects of Mg^{2+}. Most previous measurements of the kinetics of the interaction have been carried out in the presence of various concentrations of Mg^{2+} (usually ~10 mM; Riggs et al., 1970). In their analysis of the data of Riggs et al. (1970), Record et al. (1977) assumed that Mg^{2+} and K^+ bind to DNA as competitive counterions and that in mixtures of the two counterions (where [K^+] was generally varied in the presence of fixed [Mg^{2+}]) the effect of Mg^{2+} on the observed rate of RO complex formation could be corrected for directly on this basis (Lohman et al., 1978). To demonstrate that this approach is valid and that small concentrations of Mg^{2+} are not involved in other processes reflected in association rates (we recall that the association experiments are largely performed under conditions for which RO formation is effectively irreversible, and thus k_a is not dependent on the value of K_{RO}), we carried out a series of association rate experiments in the presence of varying (small) concentrations of both cations. The results, summarized in Table I, show that values of k_a measured in the presence of low concentrations of Mg^{2+}, or in mixtures of Mg^{2+} and K^+, are approximately the same.

Table I: Observed Values for k_a for *lac* Repressor Association with λ*plac*5 DNA in Low Concentrations of K^+ and Mg^{2+} [a]

[KCl] (mM)	[$MgCl_2$] (mM)	k_a (M^{-1} s^{-1}) [b]
	1	1.5×10^{10}
	10	1.4×10^{10}
10	10	1.4×10^{10}
20	1	1.3×10^{10}

[a] All experiments were performed in BB containing the indicated amounts of KCl and $MgCl_2$. [b] The standard error in these values is ~ $\pm 0.4 \times 10^{10}$ M^{-1} s^{-1}.

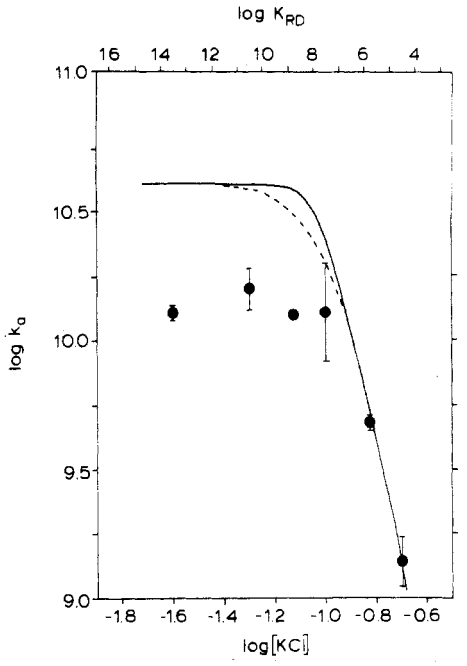

FIGURE 3: Log k_a vs. log [KCl] for RO complex formation with the *Eco*RI *lac* operator containing DNA fragments (see legend to Figure 2 for experimental details). The lines represent the theoretical predictions for the sliding mechanism as described by eq 7 and 12. The parameter values used are $D = 5 \times 10^{-7}$ cm^2/s, $M = 6700$ base pairs, $R_c = 750$ Å, $r_s = 2100$ Å, $O_T = 0.5 \times 10^{-12}$ M, and $D_1 = 9 \times 10^{-10}$ cm^2/s. The solid curve represents values of k_a calculated as a function of K_{RD} (upper abscissa) estimated using eq 13. The dashed portion is calculated assuming the weaker dependence of K_{RD} on [KCl] described in the legend to Figure 2.

Parallel stoichiometric (equilibrium) titrations [see Winter & von Hippel (1981)] carried out in binding buffer solutions containing 0.1 M KCl and no Mg^{2+}, and 10 mM KCl and 10 mM $MgCl_2$, respectively, showed that equal amounts of repressor are complexed by operator under both conditions. These findings, together with those of Barkley (1981), confirm that Mg^{2+} can generally be treated as a (appropriately weighted) competing cation in studies of the dependence of k_a on salt concentration.

Association to the EcoRI Fragment. The results of similar kinetic measurements using the *Eco*RI operator-containing DNA fragment [6700 base pairs; see Figure 1 of Winter & von Hippel (1981)] are presented in Figure 3. We see that on the "high salt" side of the plot the dependence of k_a on KCl concentration is very similar to that seen with λ*plac*5 DNA as the target lattice. Again log k_a increases directly with decreasing log [KCl] over the 0.2 to ~0.1 M salt concentration range, with k_a again increasing ~10-fold (to $\sim 2 \times 10^{10}$ M^{-1} s^{-1}) over this interval. In parallel to our findings with the λ*plac*5 DNA lattice, k_a reaches a maximum value, here at ~0.08 M KCl. However, rather than falling again with further decrease in KCl concentration, the value of k_a remains essentially constant for this operator-containing lattice as [KCl] is decreased from ~0.08 to ~0.025 M.

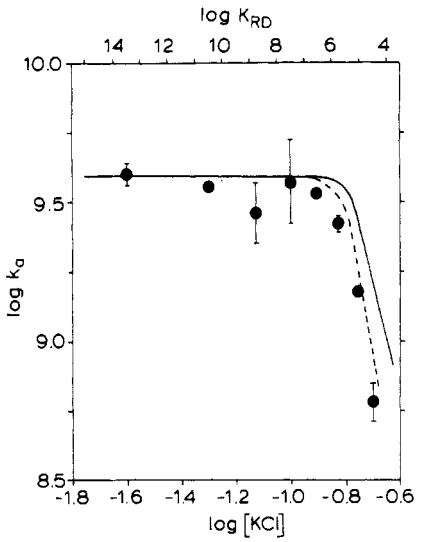

FIGURE 4: Log k_a vs. log [KCl] for RO complex formation with the *Hae*-203 *lac* operator containing DNA fragments (see legend to Figure 2 for experimental details). The lines represent the theoretical predictions for the sliding mechanism as described by eq 4. K_{RD} (calculated from eq 13) is given in the upper abscissa. The parameter values used are $D = D_R + D_0 = 6.5 \times 10^{-7}$ cm^2/s and $M = 175$ base pairs (rather than 203 to account for end effects). The solid curve here is calculated by using $D_1 = 9 \times 10^{-10}$ cm^2/s, and the dashed curve is calculated for $D_1 = 3 \times 10^{-10}$ cm^2/s.

This latter result shows that the falloff of k_a with decreasing salt concentration seen with the λ*plac*5 DNA lattice below ~0.1 M salt is *not* due to events such as protein denaturation, aggregation, or conformational change at low salt but reflects a real component of the kinetic mechanism of the association process. In addition, of course, the *disappearance* of this feature for the shorter lattices is also mechanistically significant.

Association to the Hae-203 and the (Hae + Hpa)-80 Fragment. The kinetics of the association of *lac* repressor with the small operator-containing fragment created by *Hae*III digestion [the *Hae*-203 fragment; see Figure 1 of Winter & von Hippel (1981)] have been studied in the same way, and the results are presented in Figure 4, again as a plot of log k_a vs. log [KCl]. A pattern of behavior which is qualitatively similar to that for the *Eco*RI fragment is seen, with k_a increasing with decreasing salt (to ~0.1 M KCl) and remaining approximately constant at lower salt concentrations. However, there are important quantitative differences; for this lattice the maximum value of k_a reached is only $\sim 4 \times 10^9$ M^{-1} s^{-1}, and the rate of increase of log k_a with decreasing log [KCl] is somewhat smaller than that seen with the larger lattices.

Limited measurements of association rates were also made with the 80-base-pair operator-containing fragment [(*Hae* + *Hpa*)-80] generated by digestion of the *Hae*-203 fragment with the *Hpa*II restriction enzyme [see Figure 1 of Winter & von Hippel (1981)]. The overall behavior of the RO association kinetics for this fragment (data not shown) resemble that of the *Hae*-203 fragment, except for a further decrease in the maximum value of k_a (to $\sim 2 \times 10^9$ M^{-1} s^{-1} at ≤ 0.1 M KCl).

Predictions of a One-Step Model. Before launching into a complete analysis of the preceding kinetic data in terms of the various two-step mechanisms presented in Berg et al. (1981), we must consider whether a one-step model involving free diffusion directly to the target site will do. In the absence of fairly bizarre assumptions, it is easy to reject a one-step model simply on the basis of the overall *shapes* of the curves of association rate as a function of salt concentration.

In a one-step process, salt concentration would be expected to exert a monotonic screening effect on the observed rate (Lohman et al., 1978), with k_a *increasing* slowly with increasing salt if net repulsion between the two ligands dominates (both repressor and operator carry a net negative charge) and k_a *decreasing* slowly with increasing salt if the net positive charge of the repressor binding site itself dominates the one-step electrostatic interaction [see eq 5.4–5.6, Berg et al., 1981]. The marked gyrations of k_a over a very narrow salt concentration range (Figures 2–4) as well as the steep slope of the log k_a vs. log [KCl] plots in the 0.2–0.1 M KCl range are *not* compatible with a one-step interpretation.

It is also illuminating to make some theoretical estimates of the association rate constants we might expect on the basis of a simple one-step free diffusion process, in order to determine the *magnitude* of the effects which must be explained by facilitated translocation mechanisms. To this end, we use the Debye–Smoluchowski equation to calculate the maximum value of k_a (the diffusion-limited second-order association rate constant) which could apply to this system on the basis of direct random collisional interactions. This equation can be written as

$$k_a = 4\pi\kappa f_{elec} b(D_R + D_O)N_0/1000 \qquad (4)$$

where κ is a (unitless) steric interaction factor corresponding to the fraction of the total (macroscopic) collisions that are successful, f_{elec} is a (unitless) electrostatic factor, b is the interaction radius for the reaction (in centimeters), D_R and D_O are the three-dimensional diffusion constants for R and O (in centimeters squared per second) and N_0 is Avogadro's number.

Initially setting κ and f_{elec} equal to unity and using $b \simeq 50 \times 10^{-8}$ cm (approximately the radius of the DNA double helix plus the estimated radius of the repressor), $D_R = 5 \times 10^{-7}$ cm^2/s, and $D_O \simeq 10^{-9}$ cm^2/s (for λp*lac*5 DNA; this is the estimated diffusion constant for the *entire* DNA molecule), we obtain an absolute maximum value of $k_a \simeq 10^9$ M^{-1} s^{-1}. We note that this calculated value is already a factor of 20 lower than the observed value of k_a for λp*lac*5 DNA at 0.1 M KCl (e.g., see Figure 3) and that this discrepancy becomes much more severe when we introduce reasonable values of κ. (We take f_{elec} as $\simeq 1$ in this calculation since the overall electrostatic repulsion of R and O must be at least partially offset by attraction between the positively charged N termini of the repressor subunits and the DNA phosphates primarily involved in the nonspecific binding interaction.)

Approaches to "guesstimating" values of κ are described under General Discussion (below); depending on the assumptions made, κ can range between approximately 10^{-1} and 10^{-4}. Clearly a one-step mechanism is also inadequate to account for the *magnitudes* of the observed association rates.

Finally the fact that the overall rate of reaction of repressor with small operator-containing DNA fragments is *smaller* than that with the large DNA molecules is also consistent with the requirement for facilitating mechanisms (which become less effective for short DNA molecules). Thus, in a direct one-step interaction, we would expect k_a to be *increased* 1.4–1.8-fold over the value for λp*lac*5 DNA, on the basis of the use of values of D_0 of ($\sim$2–4) $\times 10^{-7}$ cm^2/s for these small DNA fragments in eq 4. We conclude, therefore, that facilitating mechanisms are clearly needed over the entire salt concentration range to bring k_a up to the observed values and that a two-step process must be invoked.

Qualitative Predictions Based on Two-Step Mechanisms. We now ask what conclusions can be drawn qualitatively from the overall shapes of the association kinetic curves (Figures 2–4), prior to describing quantitative efforts to fit specific mechanisms as outlined in Berg et al. (1981).

We note first the rapid increase in k_a with decreasing salt concentration in the $\sim$0.2 to $\sim$0.1 M KCl range; this indicates not only that initial nonspecific binding of repressor is involved (as required in a two-step mechanism) but also that increasing K_{RD} (and thus the duration of the nonspecifically bound state) *increases* the rate of target location. This behavior also proves that facilitated translocation processes must occur while repressor is nonspecifically bound, since otherwise increasing the duration of the nonspecifically bound state would *decrease* the overall rate of target location [compare Figure 3 with Figures 4 and 5 of Berg et al. (1981)]. If such facilitated searches involve only *correlated* processes such as sliding (i.e., searches within a discrete distance along the DNA contour from the initial binding event), then a larger segment of DNA will be explored per binding event if the average *duration* of the bound state is increased (we assume the searching *rate* is approximately independent of salt concentrations; see below).

The observed decrease in k_a (for the λp*lac*5 DNA lattice) as [KCl] is decreased further is consistent with an initial diffusional association with a nonspecific site followed by a positionally correlated search process, since as the duration of each local searching event is increased beyond the optimal value (with a concomitant decrease in uncorrelated dissociation–association events per unit time), the overall rate of target location would be expected to decrease, as observed. For shorter pieces of DNA (Figures 3 and 4), this falloff at lower salt concentrations would be expected to become smaller or to vanish altogether (as observed), since an extended *correlated* search process would be expected to result in more efficient target location per binding event as the *size* of the overall target lattice decreases.

Finally we note that the qualitative fact that k_a is *not* decreased enormously for very small operator-containing DNA fragments in dilute solution is not compatible with facilitation *only* by intersegment transfer events (Berg et al., 1981). The solution behavior of the shorter DNA chains utilized should approximate that of rods for fragments shorter than (or comparable to) the persistence length of DNA ($\sim$500–600 Å at 0.1 M KCl), and thus no intersegment transfer (within one DNA molecule) would be expected for these entities.

Analysis of the RO Association Data in Terms of the Two-Step Model. We now analyze the *observed* association kinetic data for the RO interaction in order to extract the parameters of the minimum (two-step) reaction model for the large (λp*lac*5 DNA and the *Eco*RI *lac* fragment) DNAs studied. As outlined in Berg et al. (1981), our observations will be couched in terms of the following overall reaction:

$$R + O \underset{k_d}{\overset{k_a}{\rightleftharpoons}} RO \qquad (5)$$

which we have now shown must involve at least one intermediate (RD) complex. The minimal two-step model is thus

$$R + D + O \underset{k_{-1}}{\overset{k_1}{\rightleftharpoons}} RD + O \underset{k_{-2}}{\overset{k_2}{\rightleftharpoons}} RO + D \qquad (6)$$

As also derived in Berg et al. (1981), k_a can be defined in terms of the two-step model as

$$k_a = \frac{k_2 D_T K_{RD}}{1 + D_T K_{RD} + k_2 O_T/k_{-1}} \qquad (7)$$

where D_T and O_T, respectively, represent the total concentrations of nonoperator DNA sites (effectively the total number of base pairs) and operator sites and K_{RD} (equal to k_1/k_{-1}) is the nonspecific binding constant for repressor to DNA.[1] In

Table II: Parameters for the Two-Step Model for *lac* Repressor Association with λp*lac*5 DNA

[KCl] (M)	k_a ($M^{-1}s^{-1}$)	k_{-1} (s^{-1})[a]	k_{-1} (s^{-1})[b]	k_2 ($M^{-1}s^{-1}$)[c]	k_2 ($M^{-1}s^{-1}$)[d]	k_2O_T/k_{-1}[e]	k_2O_T/k_{-1}[f]
0.025	2.7×10^9	9.4×10^{-8}	1.7×10^{-4}	2.8×10^9	2.8×10^9	2.9×10^4	1.6×10^1
0.05	1.4×10^{10}	9.7×10^{-5}	5.4×10^{-3}	1.6×10^{10}	1.6×10^{10}	1.6×10^2	3.0
0.075	1.2×10^{10}	5.5×10^{-3}	4.1×10^{-2}	1.4×10^{10}	1.7×10^{10}	2.5	0.4
0.10	1.6×10^{10}	9.7×10^{-2}		1.7×10^{10}		0.2	
0.125	1.0×10^{10}	0.9		8.0×10^{10}		8.9×10^{-2}	
0.15	5.4×10^9	5.6		2.3×10^{11}		4.1×10^{-2}	
0.175	3.1×10^9	2.6×10^1		5.8×10^{11}		2.2×10^{-2}	
0.20	1.3×10^9	1.0×10^2		9.2×10^{11}		9.2×10^{-3}	

[a] Calculated from $k_{-1} = k_1(K_{RD})^{-1}$. k_1 estimated by using eq 8 as 3.1×10^6 M^{-1} s^{-1}. K_{RD} estimated from the relationship log K_{RD} = −10 log [KCl]−2.5. [b] Same as (*a*), except K_{RD} estimated from log K_{RD} = −5 log [KCl] + 2.25. [c] Calculated using eq 7; k_{-1} values calculated as in (*a*). These calculated values for k_2 should be concentration dependent since k_2O_T is expected to be independent of concentration. [d] Calculated using eq 7; k_{-1} values calculated as in (*b*). See also comment concerning the concentration dependence of k_2 in (*c*). [e] k_{-1} values calculated as in (*a*). [f] k_{-1} values calculated as in (*b*).

Table III: Parameters of the Two-Step Model for Repressor Association with the *Eco*RI *lac* DNA Fragment

[KCl] (M)	k_a ($M^{-1}s^{-1}$)	k_{-1} (s^{-1})[a]	k_{-1} (s^{-1})[b]	k_2 ($M^{-1}s^{-1}$)[c]	k_2 ($M^{-1}s^{-1}$)[d]	k_2O_T/k_{-1}[e]	k_2O_T/k_{-1}[f]
0.025	1.3×10^{10}	1.9×10^{-7}	3.5×10^{-4}	1.9×10^{10}	1.9×10^{10}	5.0×10^4	2.7×10^1
0.05	1.6×10^{10}	2.0×10^{-4}	1.1×10^{-2}	2.6×10^{10}	4.0×10^{10}	6.5×10^1	1.8
0.075	1.3×10^{10}	1.1×10^{-2}	8.4×10^{-2}	3.0×10^{10}	9.4×10^{10}	1.3	0.56
0.10	1.3×10^{10}	2.0×10^{-1}		2.0×10^{11}		0.49	
0.15	4.8×10^{10}	1.1×10^1		1.5×10^{12}		0.13	
0.20	1.4×10^9	2.0×10^2		3.5×10^{12}		3.5×10^{-2}	

[a] Calculated from $k_{-1} = k_1(K_{RD})^{-1}$. k_1 estimated from eq 8 as 6.3×10^6 M^{-1} s^{-1}. K_{RD} from log K_{RD} = −10 log [KCl]−2.5. [b] Same as (*a*) except log K_{RD} = −5 log [KCl] + 2.25. [c] Calculated using eq 7; k_{-1} values calculated as in (*a*). These calculated values for k_2 should be concentration dependent since k_2O_T is expected to be independent of concentration. [d] Calculated using eq 7; k_{-1} values calculated as in (*b*). See also comment concerning the concentration dependence of k_2 in (*c*). [e] k_{-1} values calculated as in (*a*). [f] k_{-1} values calculated as in (*b*).

eq 7 the parameters k_a, D_T, O_T, and K_{RD} represent known or measured quantities under our experimental conditions, and k_{-1} and k_2 must be deduced.

Following Berg & Blomberg (1977), we define the forward rate constant for the first step (eq 6) of the overall reaction [see Berg et al. (1981), eq 5.3] as

$$k_1 = \frac{4\pi D r_g N_0}{M\,(1000)} \left[1 - \frac{\tanh\,(\eta r_g)}{\eta r_g} \right] \qquad (8)$$

where D is the three-dimensional diffusion constant for free repressor (we use 5×10^{-7} cm^2/s), r_g is the radius of gyration of the operator-containing DNA (we use 6×10^{-5} cm for λp*lac*5 DNA and 2.2×10^{-5} cm for the *Eco*RI *lac* DNA fragment), M is the number of base pairs in the DNA molecule (50 000 for λp*lac*5 DNA and 6700 for the *Eco*RI fragment), and $\eta r_g = [(3L/r_g)/\ln\,(R_c/b)]^{1/2}$. Here R_c is the average (intradomain) distance between DNA segments (we use R_c = 1200 Å for λp*lac*5 DNA and 750 Å for the *Eco*RI *lac* fragment), and b is the radius of the DNA double helix (b = 15 Å in these calculations). R_c is calculated by using eq 4.4 from Berg et al. (1981). We note that eq 8 is simply a modified version of the Debye–Smoluchowski equation (eq 4), with the expression in brackets (in eq 8) representing a loss term; i.e., as written it is the probability that the repressor will *not* be lost from the DNA domain prior to *any* nonspecific binding. The major assumption in this calculation is that k_1 corresponds to an essentially salt-concentration-independent process; that is, the entire salt dependence of K_{RD} is assigned to k_{-1}. This assumption is experimentally justified below.

Using eq 8 to determine k_1, we calculate k_{-1} for each salt concentration as k_1/K_{RD}, with K_{RD} determined by linear extrapolation of published data (Revzin & von Hippel, 1977; deHaseth et al., 1977).[2] We then use these parameters, together with the experimental values of k_a, to estimate k_2 (k_{-2} is taken as zero in these calculations; that is, step 2 is treated as irreversible; see Materials and Methods). The results are summarized in Table II for RO complex formation with λp*lac*5 DNA and in Table III for the reaction with the *Eco*RI *lac* fragment.

Perusal of these tables shows that k_2 (the rate constant for transfer of repressor to operator from nonoperator DNA sites)[3] as well as k_{-1} increases monotonically with increasing salt concentration, in marked contrast to the behavior of k_a. Taken alone, this increase in k_2 with increasing salt would suggest that the rate at which repressor finds operator depends inversely on the lifetime of the RD complex, with weaker nonspecific binding facilitating operator location. This is true in part, but the values of k_{-1} listed in Tables II and III show that nonspecifically bound repressors will also dissociate from the

[1] All symbols used in this paper have the same meanings as in the preceding papers; for a complete glossary, see Table I in Berg et al. (1981).

[2] We note that values of K_{RD} have actually been *measured* only between ~0.10 and ~0.27 M NaCl (or KCl). The values of K_{RD} measured over this range by Revzin & von Hippel (1977), deHaseth et al. (1977), and Lohman et al. (1980) are in good agreement; in the calculations and theoretical modeling carried out in this paper, we use the relationship log K_{RD} = −10 log [KCl] − 2.5 (measured by deHaseth et al. in the same buffer and corrected to our pH and temperature) to obtain the needed values of K_{RD}. Estimates of K_{RD} by Wang et al. (1977), based on crude measurements of rates of exchange of repressor-bound DNA at low salt concentrations, together with some preliminary measurements of low salt values of K_{RD} by O'Gorman et al. (1980), suggest that the values of K_{RD} at low salt concentrations determined by extrapolation with the above relationship may be appreciably too high. To examine the effects of a possible systematic error in K_{RD} at low salt, we have used the relationship log K_{RD} = −5 log [KCl] + 2.25 to provide alternate estimates of K_{RD} (at salt concentrations below ~0.08 M KCl only). This latter relationship has been used in generating alternate estimates of k_a and related parameters at low salt concentrations in Figures 2 and 3 and in Tables II, III, VI, and VII.

[3] We note that k_2, which has been defined by the bimolecular reaction scheme (eq 6), actually represents the rate constant for an *intra*molecular reorganization process such that k_2O_T is a true monomolecular rate constant (i.e., independent of concentration).

DNA molecule as a whole at greatly increased rates as [KCl] is increased. The latter effect dominates the observed kinetics, and so the overall decrease of k_a with increasing salt concentration (at >0.1 M KCl) reflects this increased probability of dissociation from the entire DNA domain prior to operator binding as [KCl] increases. This probability of repressor loss from the domain is reflected in the (salt-dependent) ratio k_2O_T/k_{-1} from eq 7 (see Tables II and III); this term is simply the ratio of the rate of RO complex formation once repressor is nonspecifically bound to the rate of repressor dissociation from the entire DNA molecule or fragment. Thus at 0.075 M KCl, a repressor molecule nonspecifically bound to the λp*lac*5 DNA molecule will have an ~75% chance of locating the operator prior to dissociation; at 0.2 M KCl, this probability will have fallen to about 1%.

We note (Table II) that the ratio k_2O_T/k_{-1} becomes very large at low salt concentrations, indicating that nearly all the initially nonspecifically bound repressor will eventually reach the operator under these conditions. We also note that k_2 decreases with decreasing salt, becoming equal to k_a at ~0.05 M KCl for λp*lac*5 DNA (Table II). This means that at this salt concentration the second ("scanning") step becomes rate limiting and the overall association reaction slows down at still lower salt concentrations. This limit is not reached for the shorter *Eco*RI *lac* fragments in the salt range studied (Table III); thus k_a for this operator DNA is insensitive to variations in salt concentration below 0.1 M KCl (Figure 3) since diffusion of R to the DNA (step 1) continues to be rate limiting and nonspecifically bound repressors dissociate slowly (roughly on the time scale of the association reaction; see Table III).

As expected on the basis of our overall rate estimates, we find from this two-step analysis that facilitating mechanisms (reflected in step 2) do indeed greatly increase the rate at which nonspecifically bound repressor finds the operator site (within the same piece of DNA). This rate is k_2O_T, and the reciprocal of this quantity is the average transfer time. Thus for λp*lac*5 DNA, this time is less than 1 s at high salt concentrations and is even faster (less than ~100 ms) for the *Eco*RI *lac* fragment since fewer DNA sites need to be scanned. For still shorter DNAs, the time required for nonspecifically bound repressor to find the operator decreases still further, and the initial binding event becomes rate limiting (see below).

A two-step analysis of the rate of association of repressor with the *Hae*-203 *lac* DNA fragment using eq 7 can only be carried out over a limited range of salt concentrations (0.15–0.2 M KCl). At these salt concentrations, we estimate k_2 at ~5 × 10^{13} M^{-1} s^{-1}, which is ~100-fold greater than our estimates of k_2 for the large *lac* operator containing DNAs under the same ionic conditions (Tables II and III). This increase reflects the expected increase in the rate of operator location as the amount of DNA vicinal to the operator that needs to be "scanned" is decreased. At salt concentrations less than ~0.15 M KCl, the two-step analysis breaks down for these short DNA fragments. Here k_2O_T (the rate of repressor transfer to the operator) becomes very large compared to k_{-1} (the dissociation rate constant for the RD complex), and the term k_2O_T/k_{-1} dominates the denominator of eq 7. Thus this expression simplifies to

$$k_a = Mk_1 \qquad (9)$$

In practice, as indicated above, this means the second (repressor transfer to operator) step of the two-step mechanism becomes "instantaneous" on the time scale of the experiment, and the initial diffusion of repressor to the DNA fragment becomes rate limiting. Under these conditions the measured value of k_a (~4 × 10^9 M^{-1} s^{-1} over the 0.025–0.125 M KCl range; see Figure 4) yields $k_1 = 2 \times 10^7$ M^{-1} s^{-1}, which represents a reasonable diffusion-controlled rate constant (on a per base pair concentration scale) for the initial association of the *Hae*-203 *lac* fragment with repressor. The measured magnitudes of k_a for the (*Hae* + *Hpa*)-80 fragment and the lack of salt concentration dependence of this parameter between 0.05 and 0.15 M KCl suggest that the overall interaction with this fragment is also diffusion limited.

Table IV: RO Association Competition Experiments[a]

concn of competing DNA (M, in base pairs)	competitor used k_a (M^{-1} s^{-1}): intact calf thymus DNA	competitor used k_a (M^{-1} s^{-1}): sonicated calf thymus DNA
none	4.5 × 10^9	4.5 × 10^9
1.8 × 10^{-7}	6.0 × 10^8	5.2 × 10^8
1.8 × 10^{-6}	1.6 × 10^8	1.2 × 10^8
1.8 × 10^{-5}	4.3 × 10^7	

[a] In these experiments, unlabeled competing DNA was added to ^{32}P-labeled *Hae*-203 *lac* DNA fragments prior to the addition of repressor. Otherwise measurement of association rate constants was carried out for the *Hae*-203 *lac* DNA fragment in the text. These experiments were conducted in BB containing 0.1 M KCl.

We note that these *experimental* observations, taken together with eq 9, provide direct support for the initial assumption that k_1 is approximately salt concentration dependent. In addition, we point out that this measured value of k_1, which is the diffusion-limited rate constant for the interaction of repressor with a nonspecific DNA site on the *Hae*-203 fragment (note also the values of 3.1 × 10^6 and 6.3 × 10^6 M^{-1} s^{-1} calculated for the λp*lac*5 and the *Eco*RI fragments respectively; Tables II and III), represents an experimental measurement of the approximate (if we ignore hopping) *upper limit* of k_a in a one-step RO interaction. (κ is certainly smaller for formation of the specific RO than for the nonspecific RD complex.) Thus these experimental results suggest (compare with theoretical estimates based on eq 4) that the maximum measured value of the k_a exceeds the maximum value for a one-step (RO) interaction by ~10^3.

Effect of Competing (Large or Small) Nonoperator DNA on the RO Association Kinetics. In order to examine further the mechanisms of repressor–operator complex formation, we have investigated the effects on k_a of adding various concentrations of nonoperator DNA [calf thymus, either intact (10000–50000 base pairs) or sonicated (~70–240 base pairs)] to the reaction solution. The labeled target-operator-containing DNA in these experiments was the *Hae*-203 fragment, and the experiments were conducted in ~0.1 M KCl; the results are presented in Table IV.

In essence, these are rate-competition experiments as defined by Lin & Riggs (1972). Table IV shows that both the intact and the sonicated DNAs decrease the observed value of k_a in direct proportion to the concentration of added nonoperator DNA (a 10-fold increase in [DNA] decreases k_a ~5-fold). These findings are consistent with the above interpretation that step 1 (diffusion to the DNA fragment) is rate limiting for the RO association process for small operator-containing DNA molecules at salt concentrations below ~0.15 M KCl since the added DNA merely slows (by competitive binding) the arrival of the repressor at the labeled operator-containing fragments. They also support the notion that repressor translocation on the DNA fragment (following initial binding) is primarily by sliding since we would expect, if intersegment transfer were the dominant translocation mode, that the presence of substantial concentrations of small nonoperator-containing DNA fragments would effectively "catalyze" such a process via "interfragment" transfer events.

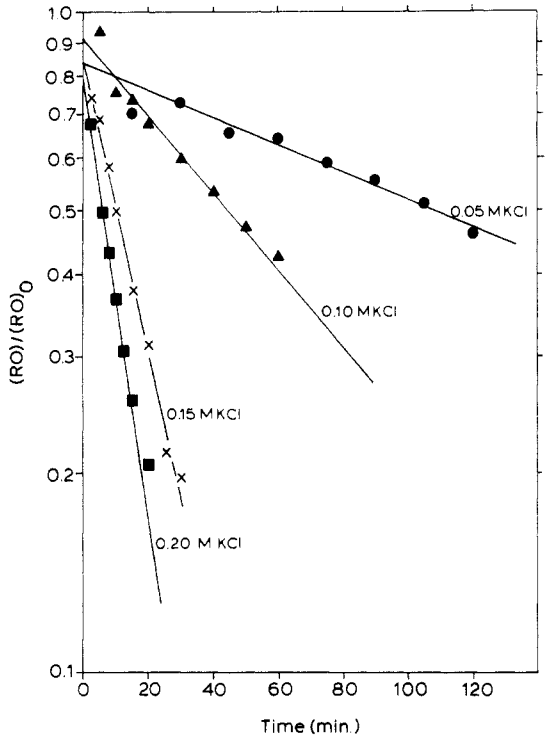

FIGURE 5: Kinetics of the dissociation of the RO complex with λp*lac*5 DNA at various salt concentrations. Experimental procedures are described under Materials and Methods. λp*lac*5 DNA concentrations were 1.7×10^{-11} M, and active repressor was added to 1×10^{-11} M. The solid lines represent the best linear least-squares fit to the data points, plotted according to eq 6. (●) BB + 0.05 M KCl, slope = $k_d = 8.0 \times 10^{-5}$ s^{-1}; (▲) BB + 0.10 M KCl, $k_d = 2.2 \times 10^{-4}$ s^{-1}; (×) BB + 0.15 M KCl, $k_d = 8.5 \times 10^{-4}$ s^{-1}; (■) 0.20 M KCl, $k_d = 1.2 \times 10^{-3}$ s^{-1}.

Repressor–Operator Dissociation Kinetics. In this section we use the same approaches and procedures developed for examining the association kinetics of the RO complex to study the rates of dissociation of this complex as a function of salt concentration (to vary K_{RD}) and operator-containing fragment length (to manipulate the quantity of nonoperator DNA directly attached to the operator site). We assume (and will demonstrate) that dissociation of the RO complex proceeds by a two-step process that is essentially the reverse of the association mechanism and that this process can also be described formally by eq 6.

The experimental procedures used in these studies are outlined under Materials and Methods and are essentially those employed by Riggs et al. (1970) in examining RO dissociation kinetics. In essence, the protocol for following the dissociation kinetics of the RO complex involves using a preequilibrated mixture of repressor and radioactive (^{32}P-labeled) operator-containing DNA and, at zero time, adding a large excess (typically 50-fold) of nonradioactive λp*lac*5 DNA. This unlabeled operator effectively "*traps*" the repressor which dissociates from the labeled RO complexes and makes the dissociation irreversible. Aliquots of the mixture are then filtered and washed at various times after addition of the "trapping" operator. Thus the decrease in labeled RO complex as a function of time reflects the kinetics of the dissociation process. It is necessary to determine whether the trapping (operator-containing) DNA plays an active role in the process; i.e., we must ask whether it actively penetrates the "domains" of the labeled DNA molecules to remove repressor or whether it can be considered an inactive "quencher" of the reaction that merely complexes repressor molecules that have dissociated from the labeled operator-containing DNA lattice. To this end we carried out control experiments involving salt-jump procedures to "quench" the reaction by manipulating the nonspecific binding affinities of the components, and thus made the dissociation reaction irreversible by essentially "passive" means. The results of these procedures are described below and show that the measured dissociation rates are indeed independent of the quenching technique under most experimental conditions used. However, under some conditions, "active" quenching (defined as a measured value of k_d which is *dependent* on quencher type or concentration) has been observed, both by us and by others (e.g., S. Bourgeois and co-workers, private communication).

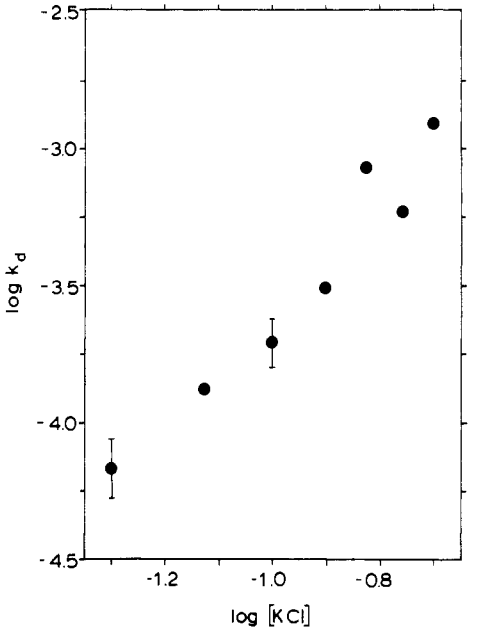

FIGURE 6: Log k_d vs. log [KCl] for RO complex dissociation from λp*lac*5 DNA. Experimental points only are shown. Operator concentration = (1–2) × 10^{-11} M; active repressor concentration = (0.5–1) × 10^{-11} M.

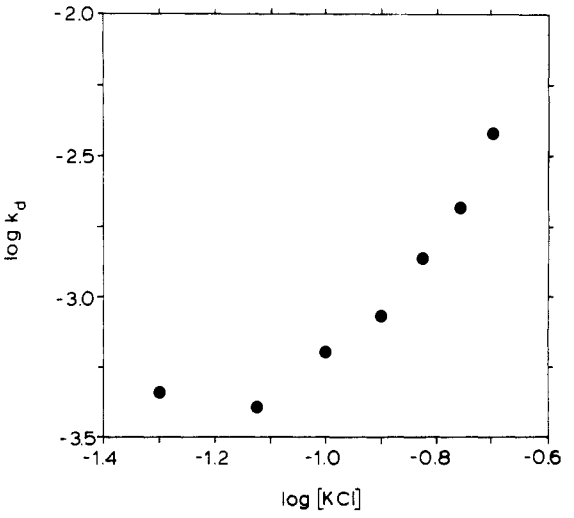

FIGURE 7: Log k_d vs. log [KCl] for RO complex dissociation from the *Hae*-203 *lac* operator containing fragment. Concentrations as in Figure 6.

Observed Repressor Dissociation Kinetics. Figure 5 shows data for the dissociation of repressor from λp*lac*5 DNA as a function of salt concentration, plotted according to eq 3. Clearly the overall dissociation process shows apparent first-order kinetics and is appreciably salt dependent. Values of the overall dissociation rate constant (k_d; eq 3) are calculated from the slopes of best-fit lines plotted as in Figure 5; values

Table V: RO Dissociation Kinetics for the *Eco*RI and (*Hae* + *Hpa*)-80 *lac* DNA Fragments[a]

[KCl] (M)	k_d (s^{-1})[b]	k_d (s^{-1})[c]
0.05	1.4×10^{-4}	2.7×10^{-4}
0.10	3.8×10^{-4}	$9.8 (\pm 0.6) \times 10^{-4}$
0.15	5.3×10^{-4}	1.6×10^{-3}
0.20	1.3×10^{-3}	$4.7 (\pm 1.3) \times 10^{-3}$

[a] In BB containing the indicated concentrations of KCl; k_d measured as described under Materials and Methods. [b] *Eco*RI *lac* DNA fragment data. [c] (*Hae* + *Hpa*)-80 *lac* DNA fragment data.

of k_d as a function of salt (KCl) concentration are then plotted as log–log plots for the λp*lac*5 DNA data in Figure 6 and for the *Hae*-203 fragment data in Figure 7. Results of similar experiments with the operator-containing *Eco*RI and the (*Hae* + *Hpa*)-80 *lac* fragments are summarized in Table V. We see that for all these systems log k_d increases directly with log [KCl] (though some flattening is seen at low salt concentrations), and the slopes of these lines give values of $\partial \log k_d/\partial \log$ [KCl] (over the 0.2–0.1 M KCl concentration range) of 2.5 (±0.5) for λp*lac*5 DNA and for the *Hae*-203 fragment, 1.7 (±0.3) for the *Eco*RI fragment, and 2.2 (±0.4) for the (*Hae* + *Hpa*)-80 fragment. (The differences between these slopes are probably not statistically significant.)

Predictions of a One-Step Dissociation Model. Figures 6 and 7 are not qualitatively inconsistent with a one-step model in that the rate constant for the RO dissociation process increases with increasing salt concentration and the magnitude of this change with salt concentration appears to be essentially independent of fragment length. Furthermore, the *magnitude* of the average slope of these data ($\partial \log k_d/\partial \log$ [KCl]) is $\sim +2.0$ (±0.7), which, coupled with the average slope for the log–log dependence of k_a on salt concentration ($\partial \log k_a/\partial \log$ [KCl]) [~ -3.3 (±0.5) over the 0.1–0.2 M KCl concentration range], is about equal to the slope of the log–log dependence of the equilibrium constant on [KCl]; i.e., $\partial \log K_{RO}/\partial \log$ [KCl] $\simeq -5.5$ (±0.6). Thus a more searching analysis is required to show that dissociation also proceeds by a two-step process (see below and General Discussion).

Analysis of the RO Dissociation Data in Terms of the Two-Step Model. We can use a similar approach to that employed with the association rate data to deduce the individual rate constants for a two-step dissociation process (eq 6), using the experimental dissociation rate data. The overall dissociation rate constant (k_d) depends on the individual rate constants of the two-step process as follows (Berg et al., 1981, eq 3.6):

$$k_d = \frac{k_{-2}D_T}{1 + k_2O_T/k_{-1} + k_{-2}D_T/k_{-1}} \quad (10)$$

where the rate constants are as defined in eq 6 and, as before, O_T and D_T represent the total concentrations of operator and nonoperator DNA sites, respectively. The parameters k_{-1} and k_2 (for the various operator-containing DNA fragments as a function of salt concentration) have been determined in the association rate analysis (above). Thus using the observed values of k_d, we can solve eq 10 for k_{-2} and for $k_{-2}D_T$ (the latter is the effective rate of dissociation of repressor from the operator site). The measured values of k_d and the rate constants calculated from these data as outlined above are summarized for receptor dissociation from λp*lac*5 DNA in Table VI and for dissociation from the *Eco*RI *lac* fragment in Table VII.

These tables show that the magnitude and salt dependence of $k_{-2}D_T$ parallels that of k_d for both these operator-containing lattices at KCl concentrations greater than ~0.1 M. Below ~0.1 M KCl, the value of $k_{-2}D_T$ increases and becomes larger than the measured value of k_d. Thus at these low salt concentrations, dissociation from the operator is no longer rate limiting since nonspecific binding becomes strong enough (i.e., RD complexes dissociate slowly enough) to reduce the overall rate of repressor release from the operator-containing DNA domain. Under most ionic conditions, however, release from the operator site is rate limiting, with release from the domain being much faster than the RO dissociation rate. This limit applies over the *entire* salt concentration range for repressor dissociation from the *Hae*-203 and (*Hae* + *Hpa*)-80 fragments, as might be expected since these moieties carry so little nonoperator DNA.

Comparison of RO dissociation rate constants as a function of operator DNA length (Figures 6 and 7 and Table V) shows an increase in k_d with decreasing length of the operator-containing DNA fragment. The hierarchy of observed dissociation rates is (*Hae* + *Hpa*)-80 ≥ *Hae*-203 > *Eco*RI *lac* > λp*lac*5 DNA. As a further comparison, we note that dissociation from 21- to 26-bp synthetic operators (Goeddel et al., 1977) is even faster than from the 80- to 203-bp fragments.

The largest incremental difference observed is the 3-fold increase in k_d seen when the length of the operator-containing

Table VI: Parameters for the Two-Step Model for *lac* Repressor Dissociation from λp*lac*5 DNA

[KCl] (M)	k_d (s^{-1})	k_{-1} (s^{-1})[a]	k_{-1} (s^{-1})[b]	$k_{-2}D_T$ (s^{-1})[c]	$k_{-2}D_T$ (s^{-1})[d]	$k_{-2}D_T/k_{-1}$[e]	$k_{-2}D_T/k_{-1}$[f]
0.05	6.8×10^{-5}	9.7×10^{-5}	5.4×10^{-3}	3.7×10^{-2}	2.8×10^{-4}	3.8×10^{2}	5.1×10^{-2}
0.075	1.3×10^{-4}	5.5×10^{-3}	4.1×10^{-2}	4.7×10^{-4}	1.8×10^{-4}	8.5×10^{-2}	4.4×10^{-3}
0.10	2.0×10^{-4}	9.7×10^{-2}		2.4×10^{-4}		2.5×10^{-3}	
0.125	3.1×10^{-4}	0.9		3.4×10^{-4}		3.7×10^{-4}	
0.15	8.5×10^{-4}	5.6		8.8×10^{-4}		1.6×10^{-4}	
0.175	5.9×10^{-4}	2.6×10^{1}		6.0×10^{-4}		2.3×10^{-5}	
0.20	1.2×10^{-3}	1.0×10^{2}		1.2×10^{-3}		1.2×10^{-5}	

[a] Calculated from $k_{-1} = k_1(K_{RD})^{-1}$. See footnote *a* of Table II. [b] See footnote *b* in Table II. [c] Calculated using eq 10; k_{-1} values calculated as in (*a*). [d] Calculated using eq 10; k_{-1} values calculated as in (*b*). [e] k_{-1} values calculated as in (*a*). [f] k_{-1} values calculated as in (*b*).

Table VII: Parameters of the Two-Step Model for *lac* Repressor Dissociation from the *Eco*RI *lac* DNA Fragment

[KCl] (M)	k_d (s^{-1})	k_{-1} (s^{-1})[a]	k_{-1} (s^{-1})[b]	$k_{-2}D_T$ (s^{-1})[c]	$k_{-2}D_T$ (s^{-1})[d]	$k_{-2}D_T/k_{-1}$[e]	$k_{-2}D_T/k_{-1}$[f]
0.05	1.4×10^{-4}	2.0×10^{-4}	1.1×10^{-2}	3.1×10^{-2}	4.0×10^{-4}	1.5×10^{2}	3.6×10^{-2}
0.10	3.8×10^{-4}	2.0×10^{-1}		5.7×10^{-4}		2.8×10^{-3}	
0.15	5.3×10^{-4}	1.1×10^{1}		6.0×10^{-4}		5.4×10^{-5}	
0.20	1.3×10^{-3}	2.0×10^{2}		1.3×10^{-3}		6.7×10^{-6}	

[a] Calculated from $k_{-1} = k_1(K_{RD})^{-1}$. See footnote *a* of Table III. [b] See footnote *b* of Table III. [c] Calculated using eq 10; k_{-1} values calculated as in (*a*). [d] Calculated using eq 10; k_{-1} values calculated as in (*b*). [e] k_{-1} values calculated as in (*a*). [f] k_{-1} values calculated as in (*b*).

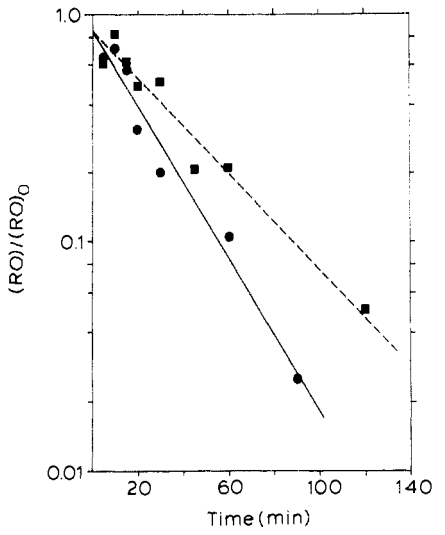

FIGURE 8: *lac* repressor dissociation from λp*lac*5 DNA as a function of "trapping" DNA size. This experiment was performed in BB containing 0.01 M KCl and 0.01 M $MgCl_2$. k_d was measured as described under Materials and Methods. (■) Trapping DNA was a 50-fold excess of unlabeled *Hae*III-digested λp*lac*5 DNA; $k_d = 4.0 \times 10^{-4}$ s^{-1}. (●) Trapping DNA was a 50-fold excess of unlabeled intact λp*lac*5 DNA; $k_d = 6.4 \times 10^{-4}$ s^{-1}.

DNA fragment is decreased from 6700 to 203 base pairs. An initially plausible interpretation is that removal of adjacent nonoperator DNA allows repressor to escape the DNA domain more rapidly, leading to a larger apparent k_d. However, since dissociation from the operator site is expected to be rate limiting (see above), we would expect that under most conditions the observed dissociation rate constant should be independent of operator-containing DNA fragment size and at very low salt the rate should be *smaller* for the small fragments, due to an increased probability of *reassociation* with the operator during the nonspecifically bound (sliding) phase of the overall dissociation process.[4]

The fact that an *increase* in k_d is observed with decreasing fragment size for the RO interaction must therefore reflect an intrinsically weaker binding of R to short operator-containing DNA fragments. In support of this interpretation, we cite the observed decreases in K_{RO} for short operator fragments observed by Winter et al. (1981) by direct equilibrium measurements [see also Goeddel et al. (1977)].

Role of the "Trapping" DNA in the Observed Dissociation Kinetics. For further examination of the nature of the RO dissociation reaction and the significance of the measured values of k_d, dissociation from ^{32}P-labeled λp*lac*5 DNA was initiated in the presence of an excess of unlabeled λp*lac*5 DNA digested with *Hae*III, and the observed dissociation rate was compared with that measured in the presence of intact λp*lac*5 DNA as "quencher" (standard conditions). The total concentration of operator used to trap repressor was identical in both experiments (a 50-fold excess over ^{32}P-labeled λp*lac*5 DNA), but the trapping (unlabeled) operator was 203-base-pairs long in the *Hae*III-cleaved sample. If the role of trapping DNA in dissociation is an active one, i.e., if it *promotes* the escape of repressor from the ^{32}P-labeled λp*lac*5 domain, then k_d should be greater for experiments in which small *lac* operator containing DNA fragments are used as "trappers". If this outcome *had* been observed, this might have reflected the penetration of small unlabeled operator-containing DNA molecules into the larger operator DNA domains with displacement of operator-bound repressor, as suggested for direct intersegment transfer processes. If, on the other hand, "trapping" DNA acts passively to prevent repressor reassociation to operator once it has dissociated, we should see little or no effect of the size of the "trapping" DNA on the measured kinetics. Figure 8 shows the latter outcome; trapping is indeed passive. In fact, dissociation in the presence of intact λp*lac*5 DNA appears to be slightly faster than when *Hae*III-digested λp*lac*5 DNA is used. Thus the trapping DNA does not, by itself, seem to promote RO dissociation.

[4] Such a dependence of the rate of dissociation on fragment size has actually been seen by Jack et al. (1980) and W. E. Jack and P. Modrich (unpublished observations) for the dissociation of *Eco*RI endonuclease from the single *Eco*RI specific binding site in pBR322 DNA (see General Discussion).

Table VIII: Dissociation of *Eco*RI *lac* Fragment RO Complexes by "Salt-Jump" Technique

KCl (concn jump) (M)	k_d (s^{-1}) obsd[a]	k_d (s^{-1}) expected[b]
0.1 to 0.4	$6.1 (\pm 0.8) \times 10^{-3}$	3.6×10^{-3}
0.1 to 0.5	$8.9 (\pm 1.4) \times 10^{-3}$	5.4×10^{-3}

[a] k_d was measured as described under Materials and Methods, except that, instead of trapping DNA, a small volume of concentrated KCl was added at zero time to initiate the irreversible dissociation process. [b] Expected values obtained from linear extrapolation of RO *lac* dissociation data in the 0.1–0.2 M KCl range (see Table VI).

Table IX: RO Association and Dissociation Kinetics for the *Hae*-170 *lac* DNA Fragment[a]

[KCl] (M)	k_d (s^{-1})	k_a (M^{-1} s^{-1})
0.025	3.7×10^{-4}	
0.05	$1.6 (\pm 0.1) \times 10^{-3}$	2.8×10^9
0.075	2.5×10^{-3}	3.0×10^9
0.10	$4.0 (\pm 0.9) \times 10^{-3}$	

[a] Containing the *Z*-gene *lac* pseudooperator; see Figure 1, Winter & von Hippel (1981). k_d was measured as described under Materials and Methods; k_a was measured by fitting the rate data to eq 5.

To initiate dissociation of preformed RO complexes *without* adding trapping DNA, we used "salt-jump" experiments of the type commonly used to measure dissociation rate in other protein–nucleic acid systems (e.g., Peterman & Wu, 1978; Lohman, 1980; Kowalczykowski et al., 1980). Repressor dissociation from the *Eco*RI *lac* fragment was measured by rapidly adding concentrated KCl to preformed RO complexes, to a final concentration of either 0.4 or 0.5 M KCl, and monitoring the resulting rate of RO complex dissociation (Table VIII). This sudden increase in [KCl] decreases K_{RO} so that specific binding can no longer be detected by the filter assay, while K_{RD} is decreased so that nonspecific binding effectively does not occur. Such an experiment should yield the "intrinsic" dissociation rate of repressor from operator at 0.4 or 0.5 M KCl. Linear extrapolation of measured values of k_d for the *Eco*RI fragment (Table VI) to 0.4 and 0.5 M KCl gives us expected k_d values at these salt concentrations (Table VIII). If the observed values of k_d in salt-jump experiments had been considerably smaller than those predicted by extrapolation of lower salt data, this would have suggested that the trapping DNA *promotes* RO dissociation in the "quenched" experiments. In fact, however, Table VIII shows good agreement (within a factor of less than 2) between the expected and observed values, implying that intrinsic operator–repressor complex dissociation rates ($= k_{-2}D_T$) are being measured under most salt concentration conditions tested.

Association and Dissociation Kinetics of Repressor lac (Z Gene) Pseudooperator. Limited kinetic measurements were carried out with the *Hae*-170 *lac* (*Z* gene) pseudooperator

fragment (Table IX). Observed values of k_a are within a factor of 2 of those measured with the *Hae*-203 and (*Hae* + *Hpa*)-80 fragments (wild-type operators). Measured values of k_d are, however, about 5-fold larger than those for the corresponding wild-type operator fragments. The binding constants for repressor to this pseudooperator DNA is ~5-fold weaker than that for repressor to wild-type operator (Winter & von Hippel, 1981), so the reduction in K_{RO} observed appears to be primarily a consequence of the increased dissociation rate. Thus, as shown above, the *amount* of vicinal nonoperator DNA, rather than details of operator base-pair sequence, is primarily responsible for determining the rate at which repressor *locates* the operator. On the other hand, the effect of an altered operator sequence (and thus altered *specific* binding) is manifested mostly in the rate of repressor release from the operator site. On this basis, other pseudooperator sites having an even weaker affinity for repressor (e.g., the *lacI* pseudooperator) might be expected to show association rates similar to those characteristic of wild-type operator, but greatly increased dissociation rates. This tends to validate measures of k_d as reflections of altered values of K_{RO} for operators of altered base-pair sequences [e.g., see Jobe et al. (1974)].

General Discussion

Summary and Overview. In this paper, we have described experiments that demonstrate unequivocally that *lac* repressor finds its target operator site within the DNA chromosome by pathways involving intermediate complexes with nonoperator DNA. We have also shown that the utilization of such two-step pathways results in a substantial (up to 10^4-fold) increase in the rate of target location over the maximum rate expected on the basis of a direct (one-step) formation of the RO complex. We have examined the overall association and dissociation kinetics of the RO interaction under a variety of experimental conditions and have analyzed the resulting rate data quantitatively to obtain estimates of the individual rate constants of the two-step process for the various operator-containing DNA lattices as a function of salt concentration. These analyses show which step is rate limiting under various conditions and allow us to approach questions of mechanism directly.

Previously, it had been pointed out (von Hippel et al., 1975) that because DNA is a high molecular weight polymer with a given intrinsic stiffness, individual DNA molecules form random coil "domains" characterized by intersegment distances and "internal" base-pair concentrations that are largely independent of total DNA concentration. As a consequence, at the great dilutions involved in kinetic experiments of the type carried out in these studies, the concentration of DNA is very nonhomogeneous in the solution. The individual DNA molecules form domains of defined size [characterized by the radius of gyration (r_g) of the molecule in solution] that occupy only a small fraction of the solution volume, with the rest of the solution remaining "empty". As described in detail by Berg et al. (1981), the process of interaction of repressor with operator under these conditions can then be represented as an initial diffusion of repressor to a DNA domain, followed by nonspecific binding to the first (nonoperator) DNA site encountered. Subsequently a given repressor molecule moves about within the DNA domain by a combination of intradomain dissociation–reassociation events and facilitated transfer mechanisms. Eventually, as a consequence of such translocation processes, the repressor either arrives at and binds to the operator or is lost from the domain entirely. The fraction of repressor molecules that take either course depends on the magnitude of K_{RD} (which depends on the salt concentration) and on the ratio of the number of specific to nonspecific sites within the domain (which, of course, depends on the quantity of nonoperator DNA per molecule).

In the first paper of this series (Berg et al., 1981), we described several processes that might be involved in repressor translocation within the DNA domain. These processes were characterized as "correlated" (hopping and sliding) or "uncorrelated" (intradomain dissociation–reassociation and intersegment transfer) events; correlated processes are defined as searches among sites located close together *along* the DNA molecule near the locus of an initial association event, and uncorrelated processes involve repressor transfer *between* DNA segments well separated from one another along the contour length of the DNA molecule. We conclude from the experiments described here (as well as those of Barkley et al., 1981) that the dominant *facilitating* process involved in repressor translocation under the experimental conditions of the filter assay are correlated in nature, demonstrating that sliding (and also hopping) together with intradomain dissociation–reassociation comprises the major pathway (step 2 of eq 6) for the transfer of repressor to operator. In the following sections we use the theory developed previously (Berg et al., 1981) to fit the experimental kinetic data quantitatively and then consider molecular implications of the various transfer mechanisms proposed.

Predictions of Theory and Comparison with Experiments. Association Kinetics. The various translocation mechanisms characterized by Berg et al. (1981) can be simply incorporated into the general two-step model defined by eq 6 and 7 via appropriate definition of the effective transfer rate of nonspecifically bound repressor to operator, k_2O_T. Thus the total rate of intersegment transfer (eq 5.9, Berg et al., 1981) is

$$k_2O_T = (\Lambda + \nu)/M \tag{11}$$

where Λ = the intradomain nonspecific dissociation rate constant, ν = the direct transfer rate constant, and M = the total number of (nonspecific) binding sites per chain. The total rate of transfer via sliding (eq 5.17, Berg et al., 1981) is

$$k_2O_T = \frac{\Lambda}{(\Lambda L^2/D_1)^{1/2} \coth (\Lambda L^2/D_1)^{1/2} - 1} \tag{12}$$

where D_1 is the diffusion constant for one-dimensional transfer (sliding) and L = one-half the contour length of the DNA chain.

The theoretical curves of log k_a vs. log K_{RO} (Figures 3–5 of Berg et al., 1981) were generated with the present results for the *lac* RO system in mind. They were calculated for the limit of a diffusion-controlled (and salt-independent) nonspecific association. If this assumption had not been made beforehand, it would follow as a necessary consequence of the theory. The agreement between prediction and experiments depends crucially on the nonspecific association being both salt independent and as fast as possible (i.e., diffusion controlled). To permit comparison with experimental data (i.e., with plots of log k_a vs. log [KCl]), we use the experimentally determined relationship between the nonspecific binding constant and the salt concentration (Revzin & von Hippel, 1977; deHaseth et al., 1977):

$$\log K_{RD} = -10 \log [KCl] - 2.5 \tag{13}$$

This expression is from deHaseth et al. (1977). It applies in Tris buffer (as used in the experiments of these papers) and has been corrected for pH and temperature. Initially we assume that this relationship (eq 13) also applies at KCl concentrations below 0.1 M, where it has not been accurately measured. However, as pointed out in footnote 2, the salt

dependence of K_{RD} at low salt is probably not as steep as specified by eq 13, and we have also used an alternate relationship to estimate K_{RD} at low salt in some calculations (see Figures 2 and 3 and Tables II, III, VI, and VII).

Long DNA Chains. In Figure 2 we compare the experimental determinations of k_a for *lac* repressor binding to λp*lac*5 DNA as a function of salt concentration with the predictions of theory. To fit the experimental data using only intersegment transfer as a facilitating (translocation) mechanism would require a transfer rate constant (ν) of 10^3 s^{-1} at ~0.1 M salt and a value approaching $\nu = 10^5$ s^{-1} in the high salt region. These values of ν are several orders of magnitude larger than the upper limit of $\nu \simeq 10^2$ s^{-1} calculated (Berg, 1979) on the basis of segmental diffusion properties of double-stranded DNA. Thus we conclude that the intersegment-transfer mechanism cannot, by itself, explain the RO association kinetics, even for long DNA chains.

In contrast, the sliding model provides an excellent fit to the experimental data (Figure 2) if we use a (salt-concentration-independent) one-dimensional diffusion constant (sliding rate constant) $D_1 \simeq 9 \times 10^{-10}$ cm^2/s. This value is physically appropriate in that it falls well below any reasonable upper limit set by hydrodynamic considerations. Thus if repressor slides linearly along the DNA (and we assume the frictional properties of the solvent near the DNA are comparable to those of the bulk solvent), D_1 should not much exceed D_3, or $\sim 5 \times 10^{-7}$ cm^2/s. If repressor maintains a fixed orientation relative to the DNA and thus rotates once around the DNA every 34 Å as it slides along the sugar–phosphate backbones, D_1 should not exceed $\sim 5 \times 10^{-9}$ cm^2/s (Schurr, 1979). Clearly the best-fit value of D_1 falls safely below these limits.

Changing the value of D_1 merely changes the predicted value of k_a in proportion to $(D_1)^{1/2}$, except at the low salt plateau where k_a changes directly with D_1 [see eq 5.19 of Berg et al. (1981)]. The various limits discussed for eq 5.19 in Berg et al. (1981) are clearly seen in Figure 2. Starting at high salt, we see that k_a increases with $(K_{RD})^{1/2}$ as the salt concentration decreases. The value of k_a goes through a maximum at $K_{RD} = 1/D_T$ (where D_T is the total concentration of DNA sites) and then decreases (with further decrease in salt concentration) with $(K_{RD})^{-1/2}$ until the low salt limit is reached at $k_a = 3D_1/(L^2O_T)$. In this limit the repressor remains bound to the DNA chain following initial binding to a nonspecific site and continues to slide over the DNA chain until the operator is found.

The discrepancy between theory and experiment near 0.05 M KCl suggests that K_{RD} is not as large at low salt as suggested by eq 13. We note (dashed curve in Figure 2) that this discrepancy is largely resolved by assuming a smaller dependence of K_{RD} on [KCl] at low salt (see footnote 2).

DNA Chains of Intermediate Length. The *Eco*RI *lac* DNA fragment (~6700 base pairs) is still long enough to form random coils with approximately spherical domains in solution. The experimental data for the RO association kinetics for this fragment are presented in Figure 3 and compared with the theoretical predictions of the two-step model utilizing sliding as the primary translocation mechanism. Again the agreement is very good in the high salt region and qualitatively reasonable at lower salt concentrations. We note that the low salt plateau is substantially higher than that observed with λp*lac*5 DNA and also that there is no longer a decrease in k_a on the low salt side of the ~0.1 M KCl maximum value of k_a. These differences reflect the different time scales of steps 1 and 2 in these different size domains. Thus, at the repressor and DNA concentrations used here, the time required to find the domains of the longer chains (λp*lac*5 DNA) is always short (over all salt conditions tested) compared to the "search time" within the domain. On the other hand, for domains of intermediate size (the *Eco*RI *lac* DNA fragment) the time to *find* the domains becomes limiting under low salt conditions.

Short DNA Chains. The *Hae*-203 fragments are so short that they can be approximately described as rods in solution. The association rate constant for such rods is given by eq 5.20 of Berg et al. (1981) as

$$k_a = 2k_{assoc}[D_1/(\Lambda l^2)]^{1/2} \tanh (\Lambda L^2/D_1)^{1/2} \quad (14)$$

In Figure 4 we see that there is excellent agreement between this prediction and the experimental results. The plateau at low salt represents the (salt-independent) rate of association of repressor to the whole chain, $k_a = Mk_{assoc} = 4\pi DL/\ln(2L/b)$ cm^3/s, which corresponds to the limit $(\Lambda L^2/D_1)^{1/2} \ll 1$ of eq 14. Also the quantitative agreement in this limit confirms the assumption that the nonspecific association is diffusion controlled.

At higher salt concentrations, the whole chain no longer serves as an effective target, and the result approaches that for the long chains when the effective target length is given by the sliding distance along the chain, $2k_{assoc}[D_1/\Lambda l^2)]^{1/2}$. This corresponds to the limit $(\Lambda L^2/D_1)^{1/2} \gg 1$ of eq 14 and means that only those repressor molecules which bind nonspecifically within $[D_1/(\Lambda l^2)^{1/2}$ base pairs of the operator have an appreciable chance of sliding to the operator site without intermediate dissociation.

Dissociation Kinetics. As discussed above, the experimental data for the dissociation process also provide strong qualitative support for a two-step kinetic scheme (eq 6), with facilitated repressor translocation occurring predominately by sliding. However, in order to use the theory of Berg et al. (1981) to make explicit (quantitative) predictions of dissociation rates, we must have independent knowledge of *both* K_{RD} and K_{RO} as a function of salt concentration, since both of these equilibrium parameters appear in the expression for k_d [see eq 3.6 and 3.9, Berg et al. (1981)]. Accurate values of K_{RD} and K_{RO} over the entire salt range are not available (see above and footnote 2 concerning low salt values of K_{RD}), and the problem for K_{RO} is compounded by the fact that this parameter is also a function of DNA fragment length [see Winter & von Hippel (1981)]. Furthermore the experimental plots of log k_d vs. log [KCl] (Figures 6 and 7) are much more monotonic than those of log k_a vs. [KCl], which also limits the conclusions that can be drawn from the comparison with theory. We have therefore not attempted to draw theoretical lines onto Figures 6 and 7 but instead limit ourselves here to a comparison of the *ratios* of k_a/k_d to K_{RO} and to a *semi*quantitative analysis of the dissociation results.

From eq 3.4, 3.5, and 3.9 of Berg et al. (1981), we can show

$$\frac{k_a}{k_d} = K_{RO}^{obsd} \frac{1 + k_2O_T/k_{-1}}{1 + (k_2O_T/k_{-1})(1 + D_TK_{RD})} = K_{RO} \frac{1 + k_2O_T/k_{-1}}{1 + D_TK_{RD} + k_2O_T/k_{-1}} \quad (15)$$

where $K_{RO}^{obsd} = K_{RO}/(1 + D_TK_{RD})$ is the observed binding constant which has not been corrected for the competitive influence of nonspecific binding. Thus, it should always hold that $K_{RO}^{obsd} < k_a/k_d < K_{RO}$. However, k_a/k_d is expected to differ from K_{RO}^{obsd} only if *both* of the following conditions apply, i.e., $D_TK_{RD} > 1$ and $k_2O_T > k_{-1}$. These conditions are fulfilled only for long DNA chains at low salt; see Tables II and III. The data of Winter & von Hippel (1981) show

reasonable agreement between K_{RO}^{obsd} and k_a/k_d for λp*lac*5 and the *Eco*RI *lac* DNA fragments at 0.1 M salt and above, as expected; reliable equilibrium measurements could not be obtained at lower salt concentrations where differences might occur. Also, as predicted from eq 15, there is reasonable agreement between K_{RO}^{obsd} and k_a/k_d for the *Hae*-203 fragments over the entire salt range studied.

The most interesting prediction of the influence of the facilitating mechanisms (sliding or intersegment transfer) on the dissociation process is that the rate constant k_d for the short operator-containing fragments should be reduced to the same extent as k_a is reduced relative to the results for the long DNA chains. Thus RO dissociation from a small fragment should be substantially slower than the longer chains, *if* the specific binding constant remains the same. Such a reduction in k_d is not observed for *lac* repressor binding to the *Hae*-203 fragments, presumably because the reduction in the specific constant with decreasing fragment size masks this effect.

It is interesting to note in this connection that a substantial decrease in k_d with decreasing fragment size *is* seen for the dissociation of *Eco*RI endonuclease from specific target sites under experimental conditions (no Mg^{2+}) that allow specific binding but not nucleolytic cleavage (Jack et al., 1980; W. E. Jack and P. Modrich, personal communication). The observed values of k_d as a function of DNA fragment size appear to follow exactly the relation expected if this protein finds its target sites by a sliding mechanism, and if the equilibrium binding constant to the target site is independent of DNA fragment length.

Conclusions. The use of sliding as the dominant mechanism for the translocation of repressor from nonspecific binding sites to the operator makes it possible to predict association rates that are in (at least) semiquantitative agreement with the kinetic data for all chain lengths and salt concentrations tested. The range of these variables examined corresponds to variations of several orders of magnitude in chain length and nonspecific binding constants, which are the major parameters of the model. This agreement has been achieved by fixing only one free parameter, the one-dimensional diffusion constant for repressor on DNA (i.e., the sliding rate) at $D_1 = 9 \times 10^{-10}$ cm^2/s. The value of D_1 corresponds to a random walk rate ($\Gamma_1 = D_1/l^2$) of 10^6 "jumps" between neighboring binding sites (base pairs) per s. The effective sliding distance during time t in such a random walk is $(D_1 t/l^2)^{1/2}$, corresponding to the "scanning" of $\sim 10^3$ base pairs in 1 s (and, of course, because of the dependence on $t^{1/2}$, of $\sim 3 \times 10^2$ base pairs in 0.1 s). The effective search distance during a nonspecific binding event is thus $[D_1(\Lambda l^2)^{1/2}$. Since the nonspecific dissociation rate constant Λ is highly salt dependent, the efficiency of the sliding mechanism also becomes salt dependent. Such a relatively fast sliding rate will completely mask any contribution from "hopping", as discussed by Berg et al. (1981), since the microscopic dissociation–reassociation events that are responsible for hopping cannot spread beyond the range that has already been searched by sliding.

The quantitative fit of theory to experiment can be somewhat improved, in some instances, if a small variation in sliding rate is allowed. Thus if D_1 is reduced to 3×10^{-10} cm^2/s for the *Hae*-203 fragments, an almost perfect match of theory and experiment is obtained over the entire binding curve. The same level of agreement can be obtained by decreasing K_{RD} slightly from the value characteristic of the longer chains. In view of the fact that K_{RO} values for these fragments are significantly different from K_{RO} values measured with the long chains (Winter & von Hippel, 1981), such small postulated changes in D_1 or K_{RD} with fragment length seem not unreasonable.

The fit of theory to experiment for long chains at salt concentrations less than ~0.1 M is less exact. As noted above, this could reflect the fact that K_{RD} is not as large at low salt as a direct extrapolation of eq 13 would suggest. The results of Wang et al. (1977) and O'Gorman et al. (1980) indicate that K_{RD} may increase at a substantially slower rate with decreasing salt (at low salt concentration) than eq 13 predicts. Since the theoretical association rates are calculated as functions of K_{RD} and then transformed to functions of salt concentration via eq 13, such a change in the variation of K_{RD} with salt would simply compress the scale (or, equivalently, stretch the curves) along the abscissa in the low salt region of Figures 2–4 (see the dashed portions of the curves in Figures 2 and 3).

This uncertainty in K_{RD} at salt concentrations below 0.1 M is a major stumbling block in the interpretation of the data in this region. However, there is also some uncertainty at higher salt concentrations since the relation used (eq 13) was, in fact, determined under somewhat different conditions, and the corrections applied are not without error. Such minor differences between the assumed and the real values of K_{RD} in the system would lead to differences in the estimate of the sliding rate required to fit the data. This uncertainty could account for some of the differences between the absolute sliding rates estimated in this study and those estimated by Barkley et al. (1981).

In contrast to the predictions of the sliding mechanism, the intersegment-transfer mechanism cannot, *by itself*, account for the absolute levels of the association rate constant, except possibly at the low salt plateaus for the longer chains (λp*lac*5 DNA and the *Eco*RI fragments). However, there is a possibility that intersegment-transfer processes contribute (together with sliding) to the overall transfer rate for the longer DNA chains. If so, the effective transfer rate should be

$$k_2 O_T = \frac{\Lambda + \nu}{[(\Lambda + \nu)L^2/D_1]^{1/2} \coth [(\Lambda + \nu)L^2/D_1]^{1/2} - 1} \quad (16)$$

from eq A19 of Berg et al. (1981). This result will differ from that of the pure sliding model (eq 12) only at low salt where the nonspecific dissociation rate constant (Λ) becomes smaller than the proposed intersegment-transfer rate constant (ν). Thus at low salt even a very small value of ν would greatly influence the predicted results for λp*lac*5 DNA. This follows because sliding becomes extremely inefficient as an operator-locating mechanism for long chains when the nonspecific dissociation rate becomes so slow that the repressor is effectively confined to the chain after initial nonspecific binding, and is thus required to slide over the entire DNA molecule in order to locate the operator. The possibility of intersegment transfer under these conditions would introduce an element of uncorrelated translocation to different parts of the chain, so that sliding along the entire contour length would not be required. Thus, if $\nu \simeq 0.1$ s^{-1} at 0.05 M salt, the gap (Figure 2) between theory and experiment at this point would be completely closed. Although highly speculative, the possibility of intersegment transfer cannot be excluded and may be important in vivo (see below). However, if this mechanism *is* involved, it must be appreciably less effective in bringing about intersegment transfer than the upper limit ($\nu \simeq 10^2$ s^{-1}) estimated from the rate of DNA segment diffusion (Berg, 1979).

Tandem Operators. The multioperator systems constructed and studied by Sadler et al. (1980) provide another check on

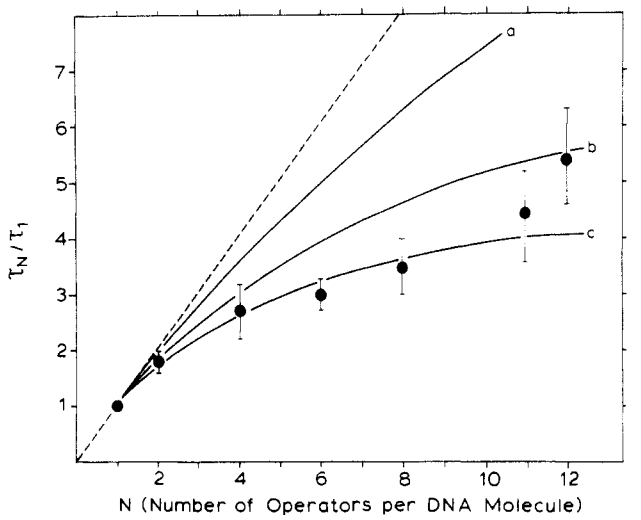

FIGURE 9: Ratio of expected mean lifetimes for the RO complex with DNA containing N tandem operators over the expected lifetime for the RO complex with DNA containing one operator vs. N [the number of tandem (identical)] operators per DNA chain, for various values of the intradomain nonspecific dissociation rate constant, Λ. (Curve a) $(\Lambda L_0^2/D_1)^{1/2} = 0.10$; (curve b) $(\Lambda L_0^2/D_1)^{1/2} = 0.25$; (curve c) $(\Lambda L_0^2/D_1)^{1/2} = 0.40$. The dashed line represents the calculated limit for $\Lambda = 0$. Data points and error bars are from Sadler et al. (1980).

the translocation mechanisms proposed for the *lac* repressor. In these experiments, Sadler et al. incorporated various numbers (from 2 to 12) of *lac* operator fragments into plasmid DNA. As discussed by Berg et al. (1981), an intersegment transfer mechanism (or no facilitated translocation mechanism at all) would predict that the effective dissociation rate constant should be independent of the number of operators present in the molecule. This is contrary to the experimental results of Sadler et al. (1980), which suggest that the repressor can transfer between operators within a single DNA molecule without being lost into the solution. Such interoperator transfer of repressor can be achieved by sliding, but not by intersegment transfer, since the operators are too close to each other to allow the necessary intermediate ring-closure events. Sliding puts strong restrictions on such interoperator transfers, since they can occur only between neighboring operators, and only via a nonspecifically bound intermediate state, in order to cross the regions of nonspecific DNA between operators located on the same DNA molecule.

We have modeled such a dissociation process in detail and find that the mean lifetime (τ_N; the inverse of the dissociation rate constant) for a repressor bound to a group of N operators can be expressed [see eq B21 of Berg et al., (1981)] as

$$\tau_N = \tau_1 \coth [\Lambda L_0^2/(4D_1)]^{1/2} \left\{ 1 - \frac{1}{N} \left[\frac{1 - \exp[-N(\Lambda L_0^2/D_1)^{1/2}]}{\sinh (\Lambda L_0^2/D_1)^{1/2}} \right] \right\} \quad (17)$$

where L_0 is the distance between operator sites. In this case L_0 is 40 base pairs, which is the center-to-center distance between adjacent operators. The result is strongly dependent on the nonspecific dissociation rate constant, Λ. In Figure 9 we have plotted the experimental data of Sadler et al. (1980), together with the predictions from eq 17 for various values of $(\Lambda L_0^2/D_1)^{1/2}$. There is excellent agreement between theory and experiment for $(\Lambda L_0^2/D_1)^{1/2} = 0.4$, which corresponds to an effective sliding distance of $[D_1/(\Lambda l^2)]^{1/2} = 100$ base pairs. This number should be compared to the estimate based on the association rate constant ($k_a = 7 \times 10^9$ M^{-1} s^{-1}) to a single operator site under the same buffer conditions (Riggs et al., 1970); from eq 5.19a of Berg et al. (1981) we obtain $k_a/2k_{assoc} = [D_1/(\Lambda l^2)]^{1/2} = 50$ base pairs. Thus the agreement between these two estimated sliding distances at a particular salt concentration is very good, considering the very different targets involved in the two cases.[5]

The predicted lifetimes from eq 17 are very salt dependent, as a consequence of the salt dependence of the nonspecific dissociation rate constant (Λ). This fact can be used as another check on the sliding model. Thus, at high salt, when the effective sliding distance becomes appreciably shorter than the distance between operators, we would expect the dissociation rate to become independent of the number of operators in the group. (To our knowledge such experiments have not yet been carried out.)

The agreement between the predictions of the sliding mechanism and the kinetic data under the widely differing conditions of our studies (involving major variation in chain length and salt concentration) and those of Barkley et al. (1981) (in which salt type and salt concentration were varied), as well as for the multioperator systems studied by Sadler et al. (1980), constitutes very strong evidence for the existence of sliding in the *lac* system.

Molecular View of Binding and Translocation Mechanisms. The Binding Process. Even the simplest of binding events is complex; this fact is reflected in the Debye–Smoluchowski equation (eq 4) in the "steric" and electrostatic parameters, κ and f_{elec}. Thus even a "diffusion-controlled" reaction does not involve just a simple encounter in which molecules strike one another once and, if the interaction sites are not exactly properly oriented, bounce away elastically. Rather, especially for large molecules, separation after an initially unsuccessful encounter is slow, and many secondary collisons occur before the molecules finally do separate. These secondary collisions occur in part because of residual (largely electrostatic) close-range attraction between the interacting molecules and in part because the random (thermally driven) motion of two closely spaced molecules of finite size has a high steric probability of bringing them back into contact. In the course of these secondary collisions, the molecules can rotate, bend, and flex in various ways. This will greatly increase the probability of bringing the potential binding sites, which may comprise only a small part of the respective molecular surfaces, into appropriate apposition for interaction. It is for this reason that reactions of this sort (e.g., enzyme–substrate binding) can be diffusion controlled, i.e., can go to completion with a probability approaching unity in the course of a single macroscopic collision. Because of the complexity of the steric rearrangements that go on during the "secondary collision" process described above, it is virtually impossible to calculate κ and f_{elec} rigorously; this would involve solving a many dimensional diffusion problem involving a multitude of undefined parameters. Crude efforts at such calculations led us to set κ at $\sim 10^{-1}$–10^{-4} (with $f_{elec} \simeq 1$) for the probability of a successful RO encounter when thermal fluctuations bring a repressor and an operator (presumably located on a short piece of DNA) within an encounter distance (b) $\simeq$ 50 Å.

Hopping. The above processes are characteristic of diffusion-driven interactions between all types of particles and, of course, underlie the deceptively simple facade of the Debye–

[5] The discrepancy between theory and experiment for $N = 12$ operators (see Figure 9) could be due to the possibility that more than one repressor molecule was bound to a group of operators at the initiation of the dissociation reaction.

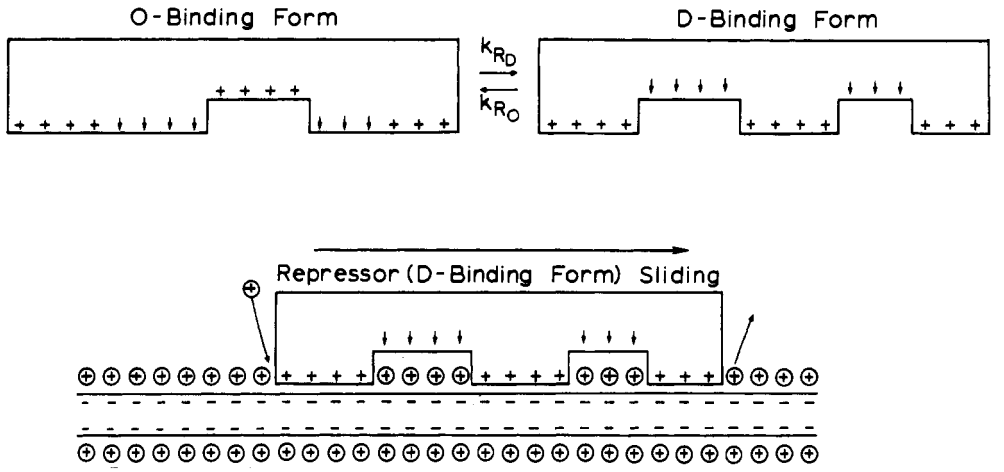

FIGURE 10: Schematic model of the operator-binding and the nonspecific DNA-binding forms of the *lac* repressor, interconverting at rates characterized by rate constants k_{R_D} and k_{R_O}. The lower model shows the nonspecific DNA-binding form sliding "through" the layer of counterions bound to the DNA molecule (see text).

Smoluchowski equation. There is one additional feature that enters in as a uniquely significant steric effect in nucleic acid–protein interactions; we have called this "hopping" (Berg et al., 1981), and it follows directly from the cylindrical geometry of the nucleic acid lattice. Thus when a protein bound to a (nonspecific) DNA site dissociates "microscopically", the probability is very high that secondary collisions will lead to multiple rebinding events at the same site. However, because of the geometry of the nucleic acid lattice, a movement of only 3.4 Å in either direction along the DNA leads to a *new* binding site; this short intersite distance leads to a nonvanishing probability that such hopping will lead to some protein translocation along the DNA lattice *during a single binding event*. We (O. G. Berg, unpublished calculations) estimate, for the *lac* repressor binding to DNA, that hopping will lead to an approximately 5–10-fold enhancement of the initial encounter target size; that is, 5–10 base pairs will be "scanned", on the average, in the course of each diffusional encounter of the protein with the DNA chain.

Sliding. This hopping process leads to some correlated (along the contour length) scanning of the DNA *as an integral part* of the initial (nonspecific) binding process. However, as is clearly apparent from the considerations discussed in this paper, a *correlated* translocation mechanism that can lead to the scanning of up to several hundred base pairs of DNA (at low salt) is required to account for the observed kinetics. This process has been termed "sliding" by us and others, and in view of its now unambiguously documented physical reality, the molecular nature of this process deserves careful examination. Any proposed sliding process must be compatible with the following facts. (i) It must be fast; i.e., the protein must be able to traverse the DNA lattice at a sliding *rate* of $\sim 10^6$ base pairs/s, i.e., at a diffusion rate of $\sim 10^{-9}$ cm^2/s or 10^7 Å^2/s (we emphasize that this is a random walk process and thus not directly akin to a velocity). (ii) It must require the input of relatively little free energy since the process must be driven by thermal fluctuations of the order of kT. (That is, movement in the sliding mode from one binding site to the next must involve a very small activation barrier.) Thus the protein must not be "site bound" in the nonspecific binding mode; rather the sliding movement *along* the DNA lattice must resemble movement along a continuous (locally "featureless") cylinder. (iii) The protein must, within a high probability, recognize a specific binding site when such a site is encountered while translocating over the DNA at the above high rate. The inferred molecular nature of the binding of repressor to nonspecific DNA, coupled with the conformational motility of the repressor molecule, fits these requirements well.

As discussed in the preceding paper of this issue (Winter & von Hippel, 1981) and described in detail in von Hippel (1979), repressor binds to the operator site by a combination of functional-group-specific hydrogen-bonding and nonspecific electrostatic interactions. When bound to nonoperator DNA, we imagine that so many of the specific hydrogen-bonding interactions used in binding to operator are "misaligned" that the repressor undergoes a conformational change to a nonoperator binding form in which electrostatic interactions are maximized (11 charge–charge interactions instead of the 6–8 characteristic of the RO complexed form) and that the operator-specific hydrogen-bonding groups are "withdrawn" from contact with the DNA. The latter (nonoperator-DNA-binding) form is ideal for sliding—the protein is held to the DNA by electrostatic attraction and can move freely on the DNA because such translocation is, in essence, movement on an isopotential surface. The binding affinity, according to the Record–Manning view of such interactions [e.g., see Record et al. (1976); Manning (1979)], is entirely due to the entropy of dilution (or mixing) of the counterions displaced from the DNA by binding of the (for these purposes) polycationic repressor. As the repressor moves along the DNA it displaces counterions from the DNA "ahead" of it, and the same number of counterions are immediately replaced on the DNA that the repressor has just "vacated". The relaxation of the ion atmosphere is rapid compared to the rate of movement of the repressor, and so the ion atmosphere is always at equilibrium. If the counterions are not totally "site bound" to the individual DNA phosphates [see Record et al. (1978)] and the positive charges on the protein are not all precisely in register with the DNA phosphates they neutralize in the RD complex, we would expect very little resistance (i.e., a very small activation barrier) to repressor sliding on the DNA. If, in addition, the rate constants for the interconversion of the operator-specific and the nonspecific DNA binding conformations are fast compared to the rate of sliding [i.e., $k_{conf} \geq 10^6$ s^{-1} for the conversion of the nonspecific to the operator-specific binding form of repressor; evidence from rapid reactions studies by Laiken et al. (1972), Wu et al. (1976), Friedman et al. (1977), etc., suggest that at least some repressor isomerizations proceed at this rate], we have all the conditions necessary to support the proposed picture of the sliding process. These notions are summarized, and illustrated schematically, in Figure 10.

Though this picture of a sliding mechanism has been developed specifically in terms of the *lac* repressor–operator-

DNA system, we believe it can readily be generalized to the kinetics of the interactions of other target-specific binding proteins with DNA and to other biological target location processes such as those involved in the movement of ligands on membrane surfaces, the location of a specific receptor on the surface of a bacterium by a phage, etc. All that is required is a general (usually electrostatic, but perhaps hydrophobic in some instances) affinity between the "target-seeking" moiety and the general (nonspecific) target surface and a rapid equilibrium between the target-specific form and a target-nonspecific form of the binding ligand. These requirements should not generally be difficult to meet.

Intersegment Transfer. Since we have not produced direct evidence for the involvement of the intersegment transfer process in the kinetics of the RO interaction on free DNA in solution, we will not dwell further on possible molecular mechanisms for that process here. In principle, all that is required is that the protein (or other ligand) to be transferred carry two (or more) potential nonspecific binding sites (von Hippel et al., 1975). Information presently available about *lac* repressor structure [see von Hippel (1979); Winter & von Hippel (1981)] indicates that this molecule very likely does carry at least two such binding sites, and the experiments of O'Gorman et al. (1980) suggest that the necessary doubly bound intermediate (RO_2) can be isolated under some conditions. Intersegment transfer mechanisms may be more important between loops of the compact DNA genomes present in vivo and will be considered further below.

In Vivo Implications of Facilitated Translocation Mechanisms. The demonstrated existence of translocation *along* the DNA chain by sliding, coupled with the possibility of translocation *between* DNA segments by the intersegment transfer mechanism, has obvious implications for the location by regulatory proteins of specific target sequences on the genome in vivo. Of course the functional genome (in both prokaryotic and eukaryotic organisms) does not consist of free randomly coiled DNA. Rather it is much more tightly packed (condensed?) as nucleoprotein complexes into chromatin (eukaryotes) or nucleoid bodies (prokaryotes). The individual loops of DNA undergoing transcription (or replication) may not involve very long stretches unencumbered by proteins or structural elements of the chromosome, and thus the mean DNA contour length available for sliding by regulatory proteins may be rather restricted. On the other hand, the close packing of DNA loops [e.g., in the *E. coli* nucleoid body; see Pettijohn & Hecht (1974); Worcel et al., 1974], which may bring DNA segments into much closer lateral proximity than the average intersegment distance (R_c) in the unperturbed DNA domain, could markedly increase the average rate of protein translocation by intersegment transfer (ν).

A more quantitative consideration of the in vivo situation in *E. coli* suggests that conditions in the cell are arranged so as to optimize the rate of genome target location (e.g., operator) by regulatory proteins (e.g., repressor) if facilitated translocation by sliding (and possibly intersegment transfer) is involved. It has been shown elsewhere, using a minicell mutant strain (Kao-Huang et al., 1977; D. Noble and P. H. von Hippel, unpublished experiments), that ~7–10% of the *lac* repressor in the cell is free in the cytoplasm and that the remainder is bound (mostly nonspecifically) to the DNA. On this basis, the intracellular value of the nonspecific binding constant (K_{RD}) can be estimated at $\sim 5 \times 10^2$ to 10^3 M^{-1}. The concentration of nonspecific binding sites in the cell is $\sim 2 \times 10^{-2}$ M ($\sim 10^7$ sites/cell; von Hippel et al., 1974); of these, up to 50% may be free and available for nonspecific repressor binding at any particular time.

For long DNA chains, the rate of transfer of repressor to operator "peaks" at a salt concentration at which $D_T K_{RD} \simeq 1$ (Berg et al., 1981); at this point the net effect of correlated "scanning" via sliding (and hopping) and of uncorrelated intradomain dissociation and reassociation and possible intersegment transfer, which work together to bring repressor to new DNA segments, maximizes the efficiency of operator location. For free λp*lac*5 DNA at an operator concentration of $\sim 10^{-12}$ M (and, since λ DNA has $\sim 5 \times 10^4$ base pairs, at a nonspecific DNA site concentration of $\sim 5 \times 10^{-8}$ M), the rate of operator location goes through a maximum at ~0.1 M KCl (Figure 2), corresponding to a value for K_{RD} of $\sim 2 \times 10^7$ M^{-1}.

As indicated above, the DNA is much more tightly packed within the *E. coli* cell (at a concentration of $\sim 10^{-2}$ M sites), and the value of K_{RD} is proportionately lower ($\sim 5 \times 10^2$ to 10^3 M^{-1}). Thus in vivo $D_T K_{RD}$ is $\simeq 10$, and the rate of genome target location is not far from optimal for a combination of correlated sliding and noncorrelated dissociation–association (possibly supplemented by intersegment transfer) mechanisms. At the same time, because of the increased effective intracellular ionic strength, the residence time on the DNA segment per nonspecific binding event, and thus the amount of DNA scanned by sliding per nonspecific binding event, are appreciably reduced. These features seem qualitatively appropriate to the structure of the genome if optimization of the rate of location of specific target sequences by genome regulatory proteins is to be maintained in vivo.

Because we know so little of the detailed organization of the functional genome and also because the effective viscosity of the intracellular medium for either one-dimensional (sliding) or three-dimensional diffusion of regulatory proteins is unknown, it is difficult to make meaningful calculations for the in vivo situation. However, some preliminary efforts, which can be modified as our knowledge of the intracellular situation increases, might not be out-of-place here. Thus, using the in vitro values of diffusion constants (i.e., $D_3 = 5 \times 10^{-7}$ cm^2/s and $D_1 = 9 \times 10^{-10}$ cm^2/s), we can calculate that the nonspecific dissociation rate constant in the cell should be approximately

$$\Lambda \simeq \frac{2\pi D l N_0}{K_{RD}(1000)} \simeq 5 \times 10^4 \text{ s}^{-1}$$

for $K_{RD} \simeq 10^3$ M^{-1}. The specific association rate in the cell is

$$k_a = \frac{k_2 D_T K_{RD}}{1 + D_T K_{RD}} \simeq k_2$$

and the average repressor–operator association time is $\tau_a = 1/(k_2 R_T)$, where $R_T \simeq 2 \times 10^{-8}$ (~10 repressors/cell).

Without translocational facilitating mechanisms, $k_a = 1.5\pi b D N_0/[1000\ (1 + D_T K_{RD})]$ (from eq 5.8, Berg et al., 1981), and the mean time for RO complex formation (for $K_{RD} \simeq 10^3$ M^{-1}) is

$$\tau_a \simeq \frac{1}{k_a R_T} \simeq 4 \text{ s}$$

This is likely to represent an appreciable underestimate, because the effective intracellular viscosity limiting three-dimensional diffusion in the cell is probably much greater than that assumed here. However, we note that an appreciable component of the fairly long association time calculated above is due to the "trapping" of repressor on nonspecific sites not located within "sliding distance" of the operator.

If we add sliding to the above model calculation, in the appropriate (long DNA chain) limit, we have (from eq 5.19c of Berg et al., 1981)

$$k_2 = 2(\Lambda D_1/l^2)^{1/2}/D_T$$

which gives an association time

$$\tau_a = \frac{D_T}{R_T}[l^2/(4\Lambda D_1)]^{1/2} \simeq 2 \text{ s}$$

for $K_{RD} \simeq 10^3$ M^{-1}. We note that while this value of τ_a is only marginally faster than that estimated for the in vivo situation without sliding, it could be greatly enhanced relative to the unfacilitated value if D_1 (the sliding rate) were less decreased from the in vitro value by intracellular viscosity effects than D_3 (the three-dimensional diffusion constant) and/or if the closer proximity of DNA loops in vivo increased the significance of intersegment transfer events. Both of these possibilities seem to us quite likely, and we conclude that probably facilitating protein translocation mechanisms of the type we have described here are required in order to avoid significant timing problems in target location by genome regulatory proteins under physiological conditions.

We are convinced that the same general principles will apply to target location by other genome regulatory proteins, e.g., of promoter sites by RNA polymerase or of replication initiation sites by DNA polymerase, etc. (Such applications will be discussed elsewhere.) Most proteins of this sort which have been examined seem to be characterized by an appreciable nonspecific binding component that is primarily electrostatic in nature (deHaseth et al., 1978; Newport et al., 1980). Thus the necessary prerequisites for facilitated protein transfer of the sort demonstrated here for *lac* repressor are at hand. Further experimental examinations of such systems, as well as others (e.g., membrane–ligand interactions) for which the studies presented in these papers may serve as a model, are eagerly awaited.

Acknowledgments

We are pleased to acknowledge many helpful discussions with Dr. John A. Schellman as these studies developed and with Drs. Robert Baldwin and Timothy Lohman on earlier versions of these manuscripts. We are also grateful to Drs. Mary Barkley, Timothy Lohman, Kathleen Matthews, Paul Modrich, Thomas Record, and John Sadler for providing us with preprints of their relevant studies prior to publication. We wish to thank Nancy Caretto for her patience, skill, and accuracy in typing and retyping the many drafts of these manuscripts and Mary Gilland for drawing the figures.

References

Barkley, M. D. (1981) *Biochemistry 20*, 3833.

Barkley, M. D., Lewis, P. A., & Sullivan, G. E. (1981) *Biochemistry 20*, 3842.

Berg, O. G. (1979) *Biopolymers 18*, 2161.

Berg, O. G., & Blomberg, C. (1977) *Biophys. Chem. 7*, 33.

Berg, O. G., Winter, R. B., and von Hippel, P. H. (1981) *Biochemistry* (first paper of three in this issue).

deHaseth, P. L., Lohman, T. M., & Record, M. T., Jr. (1977) *Biochemistry 16*, 4783.

deHaseth, P. L., Lohman, T. M., Burgress, R. R., & Record, M. T., Jr. (1978) *Biochemistry 17*, 1612.

Friedman, B. E., Olson, J. S., & Matthews, K. S. (1977) *J. Mol. Biol. 111*, 27.

Goeddel, D. V., Yansura, D. G., & Caruthers, M. H. (1977) *Proc. Natl. Acad. Sci. U.S.A. 74*, 3292.

Hinkle, D. C., & Chamberlin, M. J. (1972) *J. Mol. Biol. 70*, 157.

Jack, W. E., Rubin, R., Newman, A., & Modrich, P. (1980) *Fed. Proc., Fed. Am. Soc. Exp. Biol. 39*, 1875.

Jobe, A., Sadler, J. B., & Bourgeois, S. (1974) *J. Mol. Biol. 85*, 231.

Kao-Huang, Y., Revzin, A., Butler, A. P., O'Conner, P., Doble, D. W., & von Hippel, P. H. (1977) *Proc. Natl. Acad. Sci. U.S.A. 74*, 4228.

Kowalczykowski, S. C., Lonberg, N., Newport, J. W., Paul, L. S., & von Hippel, P. H. (1980) *Biophys. J. 32*, 403.

Laiken, S. L., Gross, C. A., & von Hippel, P. H. (1972) *J. Mol. Biol. 66*, 143.

Lin, S.-Y., & Riggs, A. D. (1972) *J. Mol. Biol. 72*, 671.

Lohman, T. M. (1980) *Biophys. J. 32*, 458.

Lohman, T. M., deHaseth, P. L., & Record, M. T., Jr. (1978) *Biophys. Chem. 8*, 281.

Lohman, T. M., Wensley, C. G., Cina, J., Burgess, R. R., & Record, M. T., Jr. (1980) *Biochemistry 19*, 3516.

Manning, G. S. (1979) *Acc. Chem. Res. 12*, 443.

Newport, J. W., Kowalczykowski, S. C., Lonberg, N., Paul, L. S., & von Hippel, P. H. (1980) in *Mechanistic Studies of DNA Replication and Genetic Recombination*, (Alberts, B. A., Ed.) pp 485–505, Academic Press, New York.

O'Gorman, R. B., Dunaway, M., & Matthews, K. S. (1980) *J. Biol. Chem. 255*, 10100.

Peterman, B. F., & Wu, S.-W. (1978) *Biochemistry 17*, 3889.

Pettijohn, D. E., & Hecht, R. (1974) *Cold Spring Harbor Symp. Quant. Biol. 38*, 31.

Record, M. T., Jr., Lohman, T. M., & deHaseth, P. L. (1976) *J. Mol. Biol. 107*, 145.

Record, M. T., Jr., deHaseth, P. L., & Lohman, T. M. (1977) *Biochemistry 16*, 4791.

Record, M. T., Jr., Anderson, C. F., & Lohman, T. M. (1978) *Q. Rev. Biophys. 72*, 103.

Revzin, A., & von Hippel, P. H. (1977) *Biochemistry 16*, 4769.

Riggs, A. D., Bourgeois, S., & Cohn, M. (1970) *J. Mol. Biol. 53*, 401.

Sadler, J. R., Tecklenburg, M., & Betz, J. L. (1980) *Gene 8*, 279.

Schurr, J. M. (1979) *Biophys. Chem. 9*, 413.

von Hippel, P. H. (1979) in *Biological Regulation and Development* (Goldberger, R. F., Ed.) pp 279–347, Plenum Press, New York.

von Hippel, P. H., Revzin, A., Gross, C. A., & Wang, A. C. (1974) *Proc. Natl. Acad. Sci. U.S.A. 71*, 4808.

von Hippel, P. H., Revzin, A., Gross, C. A., & Wang A. C. (1975) in *Protein–Ligand Interactions* (Sund, H., & Blauer, G., Eds.) pp 270–288, de Gruyter, Berlin.

Wang, A. C., Revzin, A., Butler, A. P., & von Hippel, P. H. (1977) *Nucleic Acids Res. 4*, 1579.

Winter, R. B., & von Hippel, P. H. (1981) *Biochemistry* (second paper of three in this issue).

Worcel, A., Burgi, E., Robinton, J., & Carlson, C. L. (1974) *Cold Spring Harbor Symp. Quant. Biol. 31*, 43.

Wu, Y.-H., Bandyopadhyay, P., & Wu, C.-W. (1976) *J. Mol. Biol. 100*, 459.